Micromechanics modeling of the electrical conductivity of carbon nanotube cement-matrix composites

Enrique García-Macías[a,*], Antonella D'Alessandro[b], Rafael Castro-Triguero[c], Domingo Pérez-Mira[d], Filippo Ubertini[b]

[a]*Department of Continuum Mechanics and Structural Analysis, School of Engineering, University of Seville , Camino de los Descubrimientos s/n, E-41092-Seville, Spain*
[b]*Department of Civil and Environmental Engineering, University of Perugia, Via G Duranti 93, Perugia 06125, Italy*
[c]*Department of Mechanics, University of Cordoba, Campus de Rabanales, Cordoba, CP 14071, Spain*
[d]*Department of R&D, Construcciones AZVI, Seville, Spain.*

Abstract

The incorporation of Carbon Nanotubes (CNTs) as nanoinclusions for the development of electrically conductive cement-based composites opens a vast range of possibilities for monitoring of concrete structures. A key issue for the design and optimization of these composites is the development of theoretical models capable of providing a quantitative prediction of their overall electrical conductivity. Experimental results have evidenced the strong influence of the waviness and dispersion of the nanotubes on the overall conductivity of these materials, what makes the consideration of these two phenomena essential for the development of realistic theoretical models. Nevertheless, both waviness and agglomeration have been often neglected in the literature or, when considered, have been reproduced with very simple modeling approaches not suitable to catch the complexity of the problem at hand. This paper presents an improved micromechanics model of the effective electrical conductivity of CNT cement-based nanocomposites based on enhanced approaches for reproducing waviness and non-uniform spatial distributions of the nanoinclusions. The two mechanisms that govern the electrical conductivity of these composites, electron hopping and conductive networks, are incorporated in the mixed micromechanics model. On the basis of scanning electron microscopy inspections, a helical waviness model and a two-parameter agglomeration approach are proposed. In order to assess the accuracy of the proposed analytical model, cement-based specimens have been manufactured and tested for providing data to use as the basis of comparison. In particular, specimens of cement pastes, mortars and concretes with different concentrations of Multi-Walled Carbon Nanotubes (MWCNTs) have been prepared. It is shown that the consideration of straight uniformly distributed nanotubes, as typically done in the literature, leads to an overestimation of the overall conductivity. On the contrary, it is highlighted that the wavy state of the fibers as well as their agglomeration in bundles play a crucial role in the conductivity of cement-based nanocomposites, which is demonstrated by achieving a good fit to the experimental data when using the proposed models for waviness and agglomeration. Overall, the paper highlights the physical mechanisms governing the overall electrical conductivity of cement-based composites with MWCNTs and provides a powerful analytical tool for their design.

Keywords:
Carbon nanotube, Cement-matrix composites, Electrical modeling, Percolation, Smart concrete, Structural Health Monitoring

1. Introduction

The addition of Carbon Nanotubes (CNTs) as nanoscale inclusions has attracted the interest of a large section of the scientific community due to their potential for the development of multifunctional and smart materials. Many researchers have reported the exceptional mechanical properties of CNTs with elastic modulus greater than 1 TPa [1] and ultimate tensile strength around 150 GPa [2], largely exceeding those of any previously existing material. However, the interest on CNTs is not limited to mechanical aspects but also focused on their electrical properties with conductivities between 1000 and 200000 S/cm [3], that is several orders of magnitude larger than most polymeric and cementitious materials. As a result of these properties, along with high aspect ratio, small

*Corresponding author.
Email address: egarcia28@us.es (Enrique García-Macías)

diameter, lightness and excellent chemical and thermal stability, CNTs can be used as additives to produce multifunctional composites [4]. Carbon nanotube cement-based composites are particularly interesting since concrete is one of the most employed materials for civil engineering structures. Nonetheless, the ageing processes associated with these materials make Structual Health Monitoring (SHM) essential for the assessment of the serviceability of these structures. The development of smart cement-based materials offers a large variety of possibilities for improving control, reliability and durability of the infrastructures [5–7]. Hence, the development of theoretical models capable of providing a quantitative prediction of the overall conductivity of CNT cement-based composites would be essential for the design and optimization of these nanocomposites, yet not fully achieved so far in the literature.

Due to the large disparity of mechanical and thermal properties between the cement matrix and CNTs, low CNT concentrations can substantially modify the properties of CNT cement-based composites [8, 9]. However, regarding the effective electrical properties of CNT cement-based composites, experimental measurements have demonstrated a percolation-like behavior [10–12], i.e., the conductivity varies only slightly for ranges of CNT concentrations below and above a certain critical concentration, so-called percolation threshold, at which abrupt increases are observed. Most researchers agree explaining this percolation behavior by means of two different conductive mechanisms: electron hopping at the nanoscale and conductive networks at the microscale [10, 13–15]. From quantum mechanics, electron hopping is characterized by the transfer of electrons intra-tube or from one CNT to an adjacent tube. The probability of occurrence of this mechanism is highly dependent on the distance between tubes [16, 17]. At low CNT concentrations, electron hopping governs the electrical conductivity of the composite. With increasing CNT concentration, the separation distance among CNTs decreases until adjacent fibers touch one another resulting in a continuous electrically microscale conductive path. The conductivity of composites with CNT concentrations above the percolation threshold is believed to be dominated by this second mechanism.

Most of the literature on CNT cement-based composites has focused on their fabrication process and experimental characterization. Theoretical studies coping with the explanation of the physical principles underlying the conductive mechanisms of these composites are rather scant. Among these contributions, it is noteworthy the application of lumped-circuit models of carbon fiber cement paste sensors based on series-parallel arrays of electrical resistors [18–21] and capacitors [22]. A larger number of publications is found concerning the modeling of polymeric materials doped with carbon nanotubes. Monte Carlo (MC) simulations haven been widely employed to predict the electrical conductivity of the nanocomposites [23–26]. Nevertheless, MC simulations are computationally expensive and do not offer an explicit formulation useful for design purposes. Thus, the development of analytical models has attained more attention. Traditionally, a three-parameter power law fit taken from classic percolation theory has been widely used for determining the percolation threshold [27, 28]. However, since this model requires experimental data to be fitted, it can not be used for design purposes nor let distinguish the two conductive mechanisms. Alternatively, other authors have attempted to predict the overall electrical conductivity of CNT nancomposites by means of micromechanics theory. Among them, it is worthy mentioning the work of Deng and Zheng [29] who developed a simplified micromechanics model to evaluate the effective electrical conductivity for CNT composites. This approach allowed to reproduce percolation, conductive networks, conductivity anisotropy and waviness of CNTs with good agreements with some experimental data from the literature. A similar approach was employed by Takeda et al. [30] for the analytical characterization of the electrical conductivity of carbon nanotube-based polymer composites. The predictions from the analytical model showed a good correlation with experimental results measured by alternating current impedance spectroscopy. Another relevant contribution was made by Seidel and Lagoudas [31] who proposed a Mori-Tanaka micromechanics model [32, 33] for the study of the individual influence of electron hopping and the formation of conductive networks on the electrical conductivity of CNT-polymer composites. In that work, the electron hopping mechanism was simulated by means of a conductive interphase surrounding the tubes, whilst conductive networks were represented by changes of the CNT aspect ratios. Despite the promising capabilities of this new approach, great discrepancies were observed compared to experimental data. The origin of these discrepancies was attributed by Feng and Jiang [34] to the assumption of the electrical conductivity and thickness of the interphase as constant, as well as the isolated effect of electron hopping and conductive networks before and after the percolation, respectively. These authors proposed an extension of the latter approach by considering the coupled effect of electron hopping and conductive networks on the overall conductivity with better agreement with experimental data. The simulation results also indicated that the sizes of CNTs have significant influence on the percolation threshold and, consequently, on the overall conductivity of the nanocomposites.

It should be mentioned that most of the existing theoretical studies on the electrical properties are focused on the composites with the assumption of straight conductive fillers. However, experiments have shown that most CNTs in composites present certain degree of waviness [35–37], which is due to the large aspect ratio and low bending stiffness of CNTs. In this regard, some researchers have reported on the effects of waviness on the overall

electrical properties of CNT nanocomposites. By assuming a simple sinusoidal shape, Yi at al. [38], Berhan and Sastry [39] and Fisher et al. [40] showed that CNT waviness induces considerable increases of the percolation threshold and decreases of the overall conductivity. Similar conclusions were reached by approximating wavy CNTs as elonged polygons by Li et al. [41], or by introducing equivalent straight fibers into a simplified micromechanics models, as reported by Deng and Zheng [29] and Takeda et al. [30]. A second important phenomenon that occurs in CNT composites is the agglomeration of fibers. The difficulty in obtaining good dispersion of the nanotubes is related to the circumstance that CNTs tend to form agglomerates and bundles. This phenomenon is attributed to the electronic configuration of tube walls and their high specific surface area which favors the appearance of large van der Waals' (vdW) attraction forces among nanotubes [42–44]. Although it is reported in the literature that bundles can substantially decrease the overall conductivity of the composites since they inhibit the formation of conductive networks [45], only a few contributions have attempted the theoretical simulation of this effect. Along these lines, it is worth noting the works of Weng [46] and Yang and co-authors [47]. The results showed that the inhibition of conductive networks induced by clustering leads to important increases on the percolation threshold. It is thereby essential the development of rigorous theoretical models capable of simulating waviness and clustering of CNTs for the correct comprehension of the physical principles that govern the conductivity of CNT cement-based composites, as well as for the development of effective tools for their design.

This paper presents a micromechanics model to predict the overall conductivity of CNT cement-based nanocomposites with the consideration of waviness and non-uniform spatial distributions of nanoinclusions. The two mechanisms that govern the electrical conductivity of these composites, electron hopping and conductive networks, have been incorporated in a mixed micromechanics model. The quantum tunneling effect associated with the electron hopping mechanism is simulated by means of conductive interphases surrounding the nanotubes. With regard to the conductive network mechanism, the formation of conductive paths is modeled by changes on the fiber aspect ratios. Moreover, in order to develop a more accurate model of the actual state of nanotubes within cement-based composites, the waviness and agglomeration effects are also taken into account. On the basis of Scanning Electron Microscopy (SEM) inspections, a helical waviness model and a two-parameter agglomeration approach are proposed. In order to count on an experimental basis to use as benchmark for validating the analytical results, cement-based specimens have been manufactured and characterized. In particular, specimens of cement pastes, mortars and concretes with different concentrations of Multi-Walled Carbon Nanotubes (MWCNTs) have been prepared using three preparation techniques. The first one consists of using high amount of dispersant and mechanical mixing. The two remaining strategies consider similar and lower dispersant concentrations with ultrasonic treatment. It is shown that the consideration of straight uniformly distributed nanotubes lead to an overestimation of the overall conductivity. On the contrary, it is highlighted that the wavy state of the fibers as well as their agglomeration in bundles play a crucial role in the conductivity of cement-based nanocomposites, whereby the incorporation of waviness and agglomeration effects produced a better fit to the experimental data. The proposed analytical micromechanics model is a tool that can be helpful for the twofold purpose of understanding of the physical mechanisms that govern the electrical conductivity of MWCNT cement-based composites and for assisting their design.

The paper is organized as follows. Section 2 gives a background on the micromechanics modeling of composites doped with randomly oriented straight CNTs. Section 3 presents the helical approach for the modeling of curved MWCNTs. Section 4 introduces the two-parameter model for the simulation of the agglomeration of nanoinclusions in bundles. Section 5 presents theoretical parametric studies along with comparison analyses with experimental data and, eventually, Section 6 concludes the paper.

2. Composites reinforced with randomly oriented straight CNTs

In this section, the carbon nanotubes are assumed to be straight, uniformly and randomly dispersed in the cementitious matrix. Based on the Eshelby-Mori-Tanaka mean-field homogenization framework, the electron hopping mechanism is simulated by means of a conductive interphase surrounding the tubes, whilst conductive networks are represented by changes of the CNT aspect ratios.

2.1. Tunneling resistance: Thickness and conductivity of the interphase

The electron hopping is characterized by the transfer of electrons between proximate tubes. The physical origin of this transfer is a quantum tunneling effect which defines the penetration or tunneling of an electron through a potential barrier. The transmission probability decays exponentially with the increase of the width and height of the potential barrier [48, 49]. In the case of carbon nanotube reinforced composites, the potential barrier is defined by the insulating gap of matrix d_a between proximate non-connected tubes [16, 17]. The upper limit distance for MWCNTs in conductive networks, in other words, the cut-off distance for tunneling effects, has been taken as d_c=0.5 nm [50, 51], which is the maximum possible thickness of a cementitious medium separating two adjacent

MWCNTs that allows the tunneling penetration of electrons (See Fig. 1). Due to a lack of information in the literature for estimating the average separation distance between CNTs without electrical contact, an assumption of $d_a = d_c$ has been made on this quantity in the present work. When the separation distance of CNTs is larger than d_c with CNT volume fraction f less than the percolation threshold f_c, it is regarded that CNTs are more independent rather than electrically connected to each other. In this situation, electron hopping dominates the electrical conductivity of the composite. When conductive networks are formed after percolation threshold, several works in the literature have demonstrated that the average separation distance d_a between adjacent MWCNTs follows a power-law description [30, 34, 52]. Here, we have used the expression proposed by Deng and Zheng [29]:

$$d_a = \begin{cases} d_c & 0 \le f < f_c \\ d_c \left(\dfrac{fc}{f}\right)^{1/3} & f_c \le f \le 1 \end{cases} \tag{1}$$

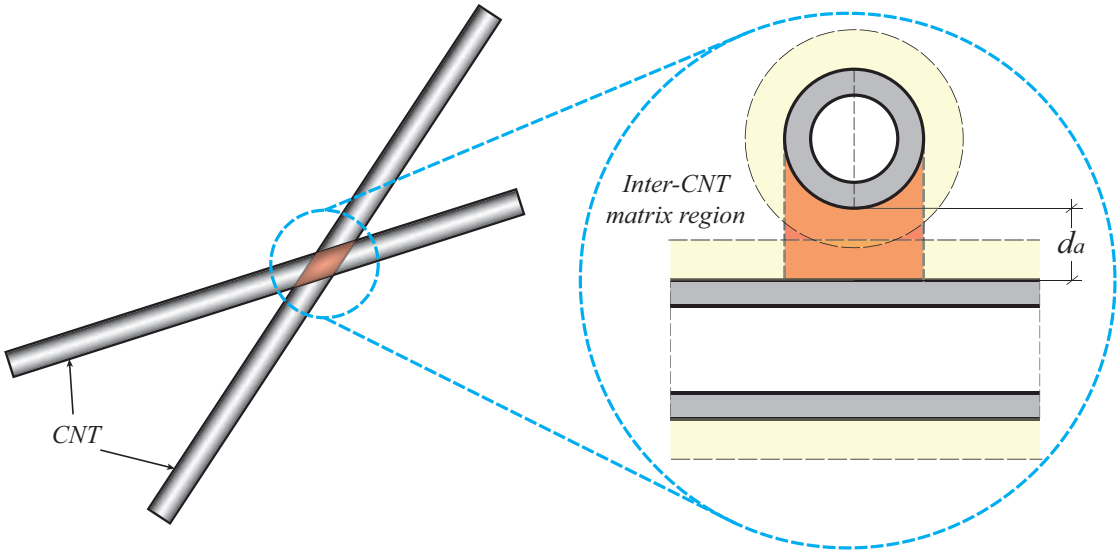

Figure 1: Contact configuration between two CNTs

Simmons [53] derived a generalized formula for the electric tunneling effect between similar electrodes separated by a thin insulating film. If we assume the thickness of insulating film in the contact area of crossing CNTs to be uniform and neglect the variation of barrier height along the thickness, the formula of the resistance to electron tunneling R_{int} for a rectangular potential barrier can be employed [54]:

$$R_{int}(d_a) = \frac{d_a \hbar^2}{ae^2 \left(2m\lambda^{1/2}\right)} \exp\left(\frac{4\pi d_a}{\hbar} \left(2m\lambda\right)^{1/2}\right) \tag{2}$$

where λ is the height of the tunneling potential barrier, m and e are the mass and the electric charge of an electron, respectively, a is the contact area of MWCNTs and $\hbar$ is the reduced Planck's constant. A reference value of 0.36eV has been taken for the height of the tunneling potential barrier based on the experimental results of Wen and Chung [50]. This effect has been incorporated into the simulation through a conductive interphase layer surrounding the nanotubes, whose thickness, t, and electrical conductivity, σ_{int}, can be expressed correspondingly as:

$$t = \frac{1}{2} d_a \tag{3}$$

$$\sigma_{int} = \frac{d_a}{aR_{int}(d_a)} \tag{4}$$

Assuming a constant average separation among MWCNTs without electrical contact may result in an overestimated electrical conductivity of the nanocomposites for MWCNT volume fraction below and around the percolation threshold. However, with the increase of CNT volume fraction the contribution of conductive networks becomes more dominating, allowing to neglect this overestimation above percolation [34].

2.2. Nanoscale composite cylinder model for CNTs

As discussed above, the electron hopping mechanism among MWCNTs distributed in the matrix has been simulated by the formation of a continuum interphase layer surrounding the nanotubes. In order to capture this interphase layer and the hollow nature of a MWCNT, an effective composite cylinder model well accepted by researchers has been used to determine the effective electrical conductivity of the MWCNT together with the surrounding interphase. Fig. 2 shows the composite cylinder assemblage which consists of a MWCNT (length L and diameter $D = 2r_c$) and the surrounding interphase with a thickness of t. In this work, MWCNTs have been treated as solid cylinders instead of a hollow tubes due to the difficulty of obtaining the actual electrical conductivity of the MWCNT considering the nanoscale structures. The effective longitudinal and transverse electrical conductivity of the cylinder, $\tilde{\sigma}^L$ and $\tilde{\sigma}^T$, respectively, can be obtained in a local coordinate system $\{x_1, x_2, x_3\}$ by applying the Maxwell's equations and the law-of-mixture rule as [34, 55]:

$$\tilde{\sigma}^L = \frac{(L+2t)\sigma_{int}\left[\sigma_c^L r_c^2 + \sigma_{int}\left(2r_c t + t^2\right)\right]}{2\sigma_c^L r_c^2 t + 2\sigma_{int}\left(2r_c t + t^2\right)t + \sigma_{int} L\left(r_c + t\right)^2} \tag{5}$$

$$\tilde{\sigma}^T = \frac{\sigma_{int}}{L+2t}\left[L\frac{2r_c^2\sigma_c^T + \left(\sigma_c^T + \sigma_{int}\right)\left(t^2 + 2r_c t\right)}{2r_c^2\sigma_{int} + \left(\sigma_c^T + \sigma_{int}\right)\left(t^2 + 2r_c t\right)} + 2t\right] \tag{6}$$

where σ_c denotes the electrical conductivity of the MWCNT and the superscripts "L" and "T" represent the longitudinal and the transverse directions, respectively. The volume fraction f_{eff} of the effective solid fillers can be obtained in terms of the volume fraction of MWCNTs f in the matrix as follows:

$$f_{eff} = \frac{\left(r_c + t\right)^2\left(L + 2t\right)}{r_c^2 L} f \tag{7}$$

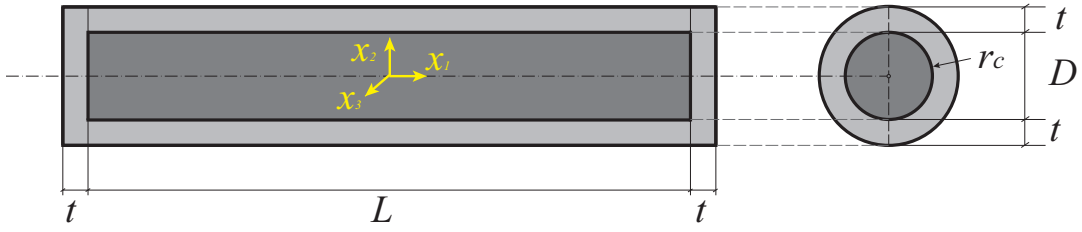

Figure 2: Equivalent composite cylinder

In this way, the composite itself is composed of two phases: the matrix and the effective solid fibers. For this two-phase composite, a micromechanics model has been applied to determine its overall electrical conductivity.

2.3. Mixed micromechanics model

Let us consider the representative volume element (RVE) of cementitious matrix doped with randomly dispersed straight MWCNTs of Fig. 3. It is assumed that the RVE contains a sufficient number of fillers in such a way that the overall properties of the composite are statistically represented. The effective properties of the RVE have been estimated by means of the electrical counterpart of the mean-field homogenization model of Eshelby-Mori-Tanaka. The Mori-Tanaka method [32] allows the extension of the theory of Eshelby [56, 57], restricted to the analysis of an isolated inclusion within a semi-infinite elastic, homogeneous and isotropic medium, to the case of multiple inhomogeneities embedded in a finite domain. The Eshelby-Mori-Tanaka approach, known as the equivalent inclusion-average stress method, is based on the equivalent elastic inclusion idea of Eshelby and the concept of average stress in the matrix due to Mori-Tanaka.

As discussed in the previous section, MWCNTs together with the surrounding interphases can be simulated as equivalent solid fillers. The orientation of a straight filler aligned in the local x_1 direction is characterized by two Euler angles φ and ψ, as shown in Fig. 3. According to the non-interacting inclusions assumption of the Mori-Tanaka method, the effective electric conductivity $\boldsymbol{\sigma}_{eff}$ of the nanocomposite can be determined by averaging over all possible orientations of the fillers in the RVE according to the following expression [58]:

$$\boldsymbol{\sigma}_{eff} = \boldsymbol{\sigma}_m + f_{eff}\frac{\int_0^{2\pi}\int_0^{\pi} ODF(\varphi,\psi)\left(\boldsymbol{\sigma}_{cnt} - \boldsymbol{\sigma}_m\right)\boldsymbol{A}\sin(\varphi)\,\mathrm{d}\varphi\mathrm{d}\psi}{\int_0^{2\pi}\int_0^{\pi} ODF(\varphi,\psi)\sin(\varphi)\,\mathrm{d}\varphi\mathrm{d}\psi} \tag{8}$$

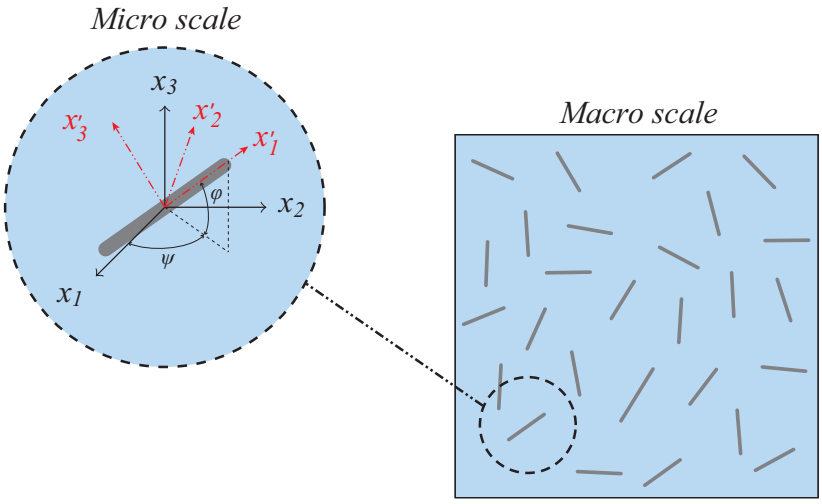

Figure 3: Representative volume element (RVE) including straight CNTs.

where $ODF(\varphi, \psi)$ is the orientation distribution function; f_{eff} is the effective volume fraction of the equivalent filler defined in Eq. (7); $\boldsymbol{\sigma}_{cnt}$ and $\boldsymbol{\sigma}_m$ are the electrical conductivity tensors of the effective filler and the matrix, respectively; and $\boldsymbol{A}$ is the electric field concentration tensor. In the case of completely random oriented fillers, the orientation distribution function ODF equals unity. The base vectors e_i and e'_i of the global (x_1, x_2, x_3) and the local coordinate systems (x'_1, x'_2, x'_3) are related via the transformation matrix $\boldsymbol{Q}$:

$$e_i = Q_{ij} e'_j \tag{9}$$

where $\boldsymbol{Q}$ is given by

$$\boldsymbol{Q} = \begin{bmatrix} \cos\psi \sin\varphi & \sin\psi \sin\varphi & \cos\varphi \\ -\sin\psi & \cos\psi & 0 \\ -\cos\psi \cos\varphi & -\sin\psi \cos\varphi 0 & \sin\varphi \end{bmatrix} \tag{10}$$

Each straight MWCNT is modeled as an equivalent solid cylinder with transversely isotropic electrical conductivity tensor in the local coordinate system, $\boldsymbol{\sigma}'_{cnt}$, given as [31]:

$$\boldsymbol{\sigma}'_{cnt} = \begin{bmatrix} \tilde{\sigma}^L & 0 & 0 \\ 0 & \tilde{\sigma}^T & 0 \\ 0 & 0 & \tilde{\sigma}^T \end{bmatrix} \tag{11}$$

with $\tilde{\sigma}^L$ and $\tilde{\sigma}^T$ being the longitudinal and transverse electrical conductivity of the effective filler as obtained in Eqs. 5 and 6, respectively. Based on the assumption of uniform and random distribution of fillers, the electric field concentration tensor $\boldsymbol{A}$ in the global coordinate system can be expressed as [34]:

$$\boldsymbol{A} = \boldsymbol{Q}^T \tilde{\boldsymbol{T}} \boldsymbol{Q} \left\{ \left(1 - f_{eff}\right) \boldsymbol{I} + \frac{f_{eff}}{4\pi} \int_0^{2\pi} \int_0^{\pi} \left\{ \boldsymbol{Q}^T \tilde{\boldsymbol{T}} \boldsymbol{Q} \right\} \sin(\varphi) \, \mathrm{d}\varphi \mathrm{d}\psi \right\}^{-1} \tag{12}$$

where

$$\tilde{\boldsymbol{T}} = \left\{ \boldsymbol{I} + \boldsymbol{S} (\boldsymbol{\sigma}_m)^{-1} (\tilde{\boldsymbol{\sigma}} - \boldsymbol{\sigma}_m) \right\}^{-1} \tag{13}$$

with $\boldsymbol{I}$ and $\boldsymbol{S}$ being the second-order identity tensor and the Eshelby tensor of the effective filler, respectively. The Eshelby tensor of a prolate spheroid ($a_2 = a_3 < a_1$) aligned in the x'_1 direction is given by [59]:

$$\boldsymbol{S} = \begin{bmatrix} S_{11} & 0 & 0 \\ 0 & S_{22} & 0 \\ 0 & 0 & S_{33} \end{bmatrix} \tag{14}$$

where

$$S_{22} = S_{33} = \frac{A_{re}}{2\left(A_{re}^2 - 1\right)^{3/2}} \left[A_{re} \left(A_{re}^2 - 1\right)^{1/2} - \cosh^{-1} A_{re} \right] \tag{15a}$$

$$S_{11} = 1 - 2S_{22} \tag{15b}$$

with A_{re} being the aspect ratio of the effective filler, i.e., A_{re}=$(L + 2t)/(D + 2t)$.

As mentioned before, several experiments and simulations have demonstrated that CNT-cement nanocomposites have a percolation-like behavior displaying a sharp increase in the electrical conductivity after the CNT volume fraction reaches a certain threshold [10–12]. For a two-phase nanocomposite with a uniformly random distribution of CNTs, the percolation threshold, f_c, can be approximately determined by the following analytical expression [29, 60]:

$$f_c(H) = \frac{9H(1-H)}{2+15H-9H^2}; \quad H = \frac{1}{A_r^2-1}\left[\frac{A_r}{\sqrt{A_r^2-1}}\ln\left(A_r+\sqrt{A_r^2-1}\right)-1\right] \tag{16}$$

where A_r is the aspect ratio of the MWCNT, i.e., $A_r = L/D$. The percolation threshold f_c denotes the onset of the percolation process. Before this critical value, $f < f_c$, electron hopping is the only mechanism that contributes to the electrical conductivity. Nonetheless, once percolation starts, $f = f_c$, a certain number of MWCNTs begin to be electrically connected forming conductive networks. Hence, for volume fractions above the percolation threshold, a percentage of MWCNTs, ξ, are connected forming conductive networks whilst the rest, $1 - \xi$, are not yet connected and only electron hopping contributes to the overall conductivity of the composite. According to Deng and Zheng [29], the relative amount of percolated MWCNTs, ξ, can be approximately estimated as:

$$\xi = \begin{cases} 0 & 0 \le f < f_c \\ \dfrac{f^{1/3}-f_c^{1/3}}{1-f_c^{1/3}} & f_c \le f \le 1 \end{cases} \tag{17}$$

From the above analysis, it is concluded that both electron hopping (EH) and conductive networks (CN) contribute to the electrical conductivity of the composite after percolation, while only electron hopping takes place before this critical value. Therefore, the expression of the overall electrical conductivity of CNT-cement nanocomposites from Eq. (8) can be extended by the sum of both mechanisms as follows:

$$\boldsymbol{\sigma}_{eff} = \boldsymbol{\sigma}_m + \boldsymbol{\sigma}_{N,EH} + \boldsymbol{\sigma}_{N,CN} \tag{18}$$

where $\boldsymbol{\sigma}_{N,EH}$ and $\boldsymbol{\sigma}_{N,CN}$ denote the electrical conductivity provided by electron hopping and conductive network mechanisms, respectively, and are defined as:

$$\boldsymbol{\sigma}_{N,EH} = (1-\xi)\frac{1}{4\pi}\int_0^{2\pi}\int_0^{\pi}\left\{f_{eff}\left(\boldsymbol{\sigma}_{EH}-\boldsymbol{\sigma}_m\right)\boldsymbol{A}_{EH}\right\}\sin(\varphi)\,\mathrm{d}\varphi\mathrm{d}\psi \tag{19}$$

$$\boldsymbol{\sigma}_{N,CN} = \xi\frac{1}{4\pi}\int_0^{2\pi}\int_0^{\pi}\left\{f_{eff}\left(\boldsymbol{\sigma}_{CN}-\boldsymbol{\sigma}_m\right)\boldsymbol{A}_{CN}\right\}\sin(\varphi)\,\mathrm{d}\varphi\mathrm{d}\psi \tag{20}$$

In the case of MWCNTs forming conductive networks, several adjacent fibers are electrically connected resulting in a continuous conductive path. This effect can be modeled by considering infinite aspect ratio of the MWCNTs as proposed by Seidel and Lagoudas [31]. Therefore, quantities associated with electron hopping correspond to the real MWCNTs aspect ratio ($a_2 = a_3 = r_c, \quad a_1 = L$), while quantities related to conductive networks correspond to an infinite aspect ratio ($a_2 = a_3 = r_c, \quad a_1 \to \infty$).

3. Composites reinforced with randomly oriented curved CNTs

In order to support the development of the analytical micromechanics model of electrical conduction in CNT cement-matrix composites, morphological analyses have been carried out on water suspensions and cementitious materials doped with MWCNTs, appropriately realized with different dispersing procedures. The results have shown that most MWCNTs in cement-based composites exist in a curved state, what is attributed to their low bending stiffness due to the small tube diameter (10-15 nm). Figure 4 shows two examples of scanning electron microscope (SEM) images, at the same magnification, of MWCNTs in water suspensions obtained after sonication by use of lignosulfonic acid sodium salt (SLS) dispersant (Fig. 4(a)), and using just mechanical mixing without dispersant (Fig. 4(b)). The micrographs show a homogeneous dispersion of the carbon fillers in the sonicated mix and the presence of visible bundles in the mechanically mixed one. Experimental investigations have also concerned the influence of different amounts of dispersant on the morphology of the MWCNTs in the water suspensions after mixing. Figure 5 shows the SEM images of MWCNTs dispersed in water solution realized with surfactant added in the concentrations of 1:1 (Fig. 5(a)) and 10:1 (Figs. 5(b) and 5(c)) with respect to the mass of the carbon nanotubes. The addition methods used for the dispersions were sonication (Figs. 5(a) and 5(b)) and

mechanical mixing (Fig. 4(c)). All the SEM images of the MWCNT-added water suspensions, realized for the dispersion analyses, have demonstrated that the carbon nanotubes exhibit similar characteristic curved geometries.

From this analysis, it can be extracted that the geometry of curved MWCNTs can be approximated by a helical curve. The geometry of this curve (Fig. 6) is defined by the diameter D_h, the spiral angle θ and the polar angle δ. The length L^{wavy} of the curved CNT is defined by these parameters as:

$$L^{wavy} = \frac{\delta D_h}{2\cos\theta} \tag{21}$$

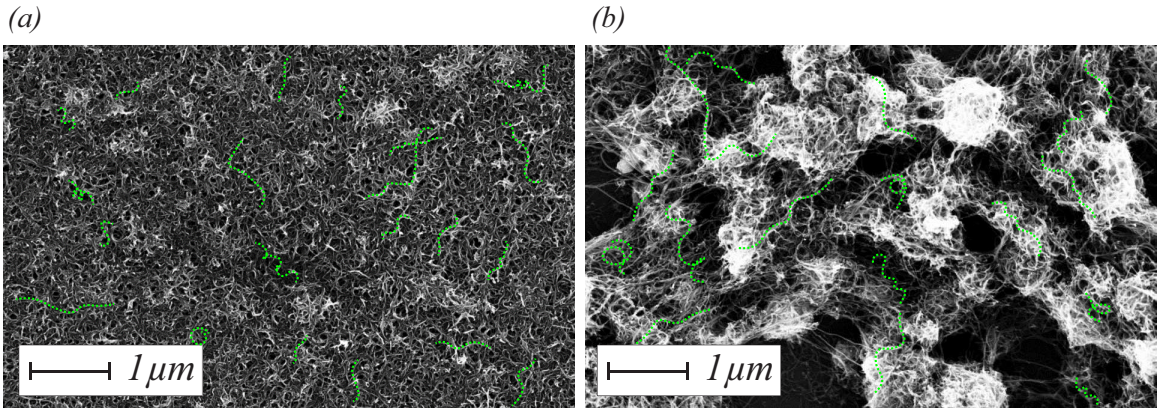

Figure 4: SEM pictures of MWCNTs in aqueous suspensions with physical dispersant after sonication (a) and without dispersant after mechanical mixing (b). (The green dashed lines represent some of the helical wavy geometries detected in the inspections).

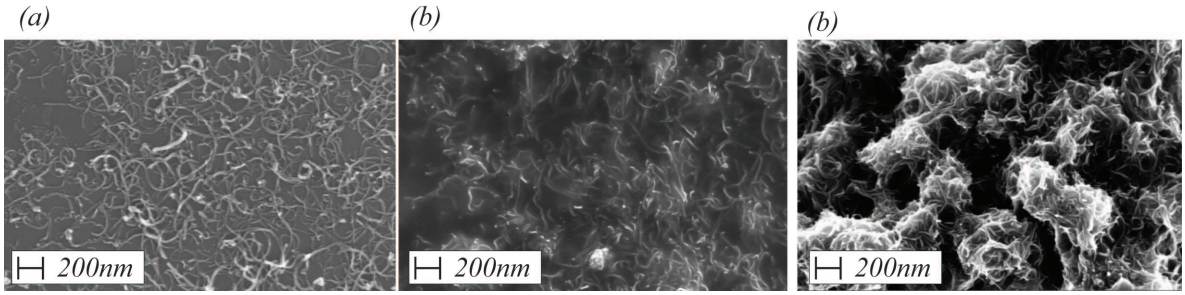

Figure 5: SEM pictures of MWCNTs in aqueous suspensions sonicated with the SLS dispersant in the 1:1 (a) and 10:1 (b) amounts, and mechanically mixed using the SLS dispersant in the 10:1 amount (c).

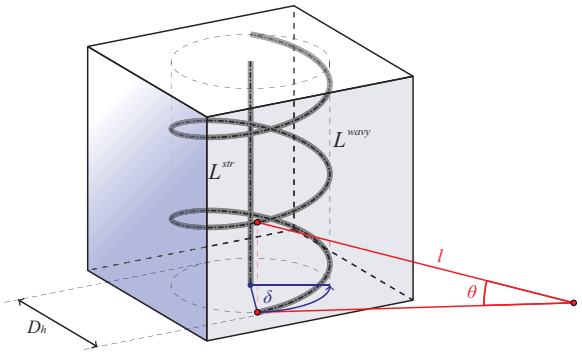

Figure 6: Helical model of a curved MWCNT and its equivalent straight counterpart.

The waviness of a MWCNT is governed by its spiral angle, θ. For example, $\theta = \pi/2$ corresponds to a straight configuration, while $\theta = 0$ corresponds to a circular MWCNT. The consideration of the waviness effect into the micromechanics modeling requires the conversion of the wavy CNTs into equivalent straight fillers of length L^{str}

[29, 30, 61]. A wavy MWCNT can be regarded as an equivalent straight fiber with the capability of (i) conducting the same electric flux J; and (ii) transporting the same amount of electric charges [34]. When the wavy MWCNT is subjected to a potential difference ΔV, the electrical flux J can be approximated by [29]:

$$J = \sigma_c^{wavy} \frac{\Delta V}{L^{wavy}} \tag{22}$$

Hence, the first condition (i) defines the effective electrical conductivity of the equivalent straight MWCNT as:

$$\sigma_c^{str} = \alpha \sigma_c^{wavy} \tag{23}$$

with $\alpha = L^{str}/L^{wavy} = \sin\theta$ the length ratio. The second condition (ii) imposes the same electrical charge through the wavy and the equivalent straight fillers and, thus, the same electrical resistance:

$$R_{cnt}^{str} = R_{cnt}^{wavy} \tag{24}$$

The combination of Eqs. (23) and (24) results in a condition of equal diameters for the wavy and the straight fillers, $D^{str} = D^{wavy}$. Finally, due to the reduction of the MWCNTs length from L^{wavy} to L^{str}, the volume fraction of the fillers must be updated to $f^{str} = \alpha f^{wavy}$, with f^{wavy} being the volume fraction of the wavy MWCNTs.

4. Agglomeration of CNTs: Two-parameter model for agglomeration

The large surface area of MWCNTs originates substantial van der Waals' attraction forces what makes MWCNTs easy to form agglomerates in bundles [35, 62]. The resulting spatial distribution of nano-inclusions within the matrix is non-uniform, so some local regions present higher concentrations of MWCNTs than the average in the composite. Fig. 7 shows two SEM pictures of MWCNTs dispersed in water solution with low content of dispersant after sonication, taken with magnification factors of 5000 and 1000, respectively. They clearly illustrate some typical carbon nanotube agglomerations occurring in aqueous suspensions, whose geometry can be approximately defined as ellipsoidal. Hence, in order to include the agglomeration effect in the proposed micromechanics approach, the bundles are assumed as ellipsoidal inclusions ($a_2 = a_3 \neq a_1$) with distinct conductive properties from the surrounding material (see Fig. 8). To this end, a two parameter agglomeration model introduced by Shi et al. [63] for the mechanical characterization of CNT-reinforced polymers, has been adapted in this work to model the conductivity of non-uniformly distributed MWCNT reinforced cement composites.

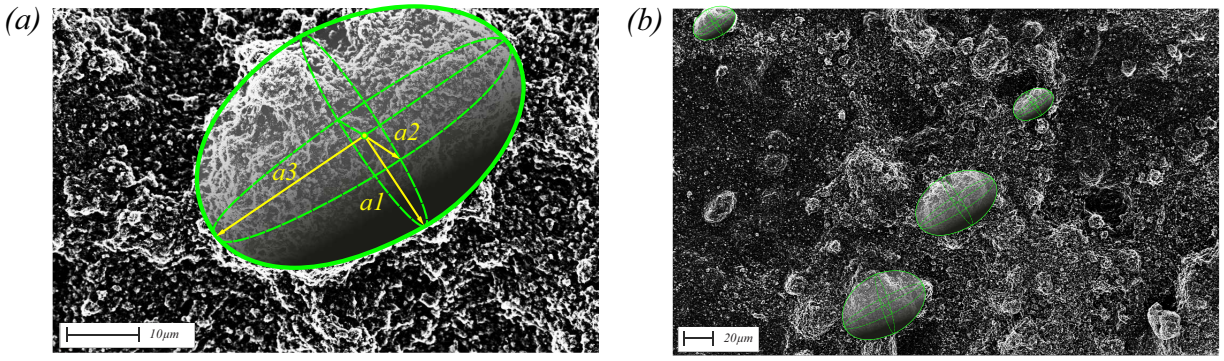

Figure 7: SEM pictures of MWCNTs in aqueous suspension with magnification factors of 5000X (a) and 1000X (b).

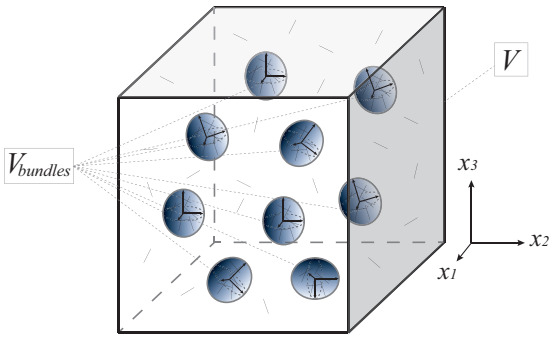

Figure 8: Sketch of RVE with ellipsoidal bundles of CNTs

The total volume V_r of CNTs in the RVE can be divided into the following two parts:

$$V_r = V_r^{bundles} + V_r^m \tag{25}$$

where $V_r^{bundles}$ and V_r^m denote the volumes of CNTs agglomerated in the bundles and dispersed in the matrix, respectively. In order to characterize the agglomeration of CNTs in the bundles, two parameters χ and ζ are introduced:

$$\chi = \frac{V_{bundles}}{V}, \quad \zeta = \frac{V_r^{bundles}}{V_r} \tag{26}$$

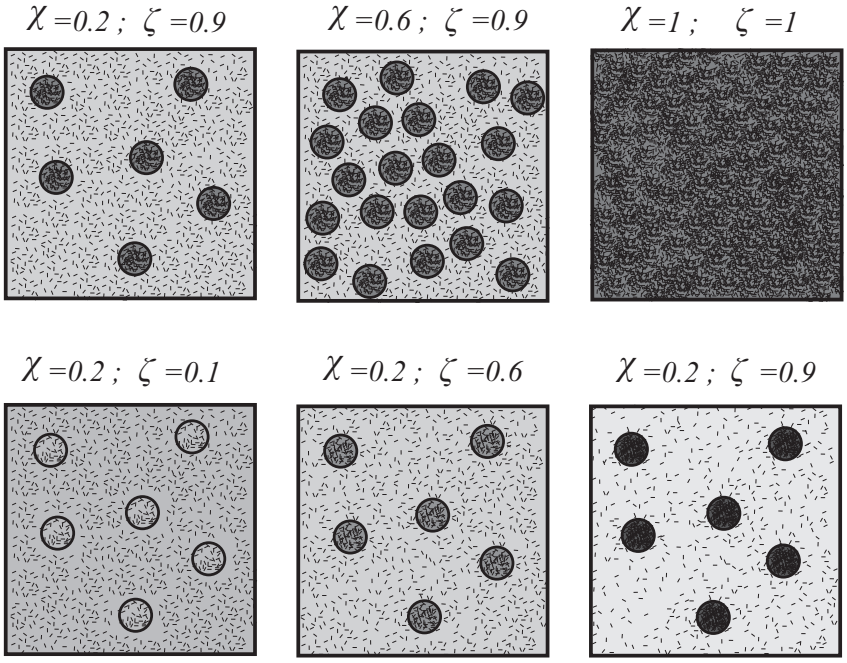

Figure 9: Schematic illustration of the variation of the parameters χ and ζ of the two-parameter agglomeration model

with $V_{bundles}$ being the volume of bundles in the RVE, ans χ the volume ratio of the bundles with respect to the total volume V of the RVE (see Fig. 8). When χ=1, nanotubes are uniformly dispersed in the matrix, and with decreasing values of χ the agglomeration degree of CNTs is more severe. The parameter ζ denotes the volume ratio of nanotubes that are dispersed in bundles and the total volume of nanotubes. In the limit case of ζ=1, all the nanotubes are located in the bundles (see Fig. 9). In the case where all nanotubes are dispersed uniformly, one has that χ=ζ. The bigger the value ζ with $\zeta > \chi$, the more heterogeneous is the spatial distribution for CNTs.

The homogenization procedure defined in Eq. (18) has been therefore applied in two steps: inside the bundles and in the surrounding matrix. The homogenization of these two new phases has been carried out taking into account the ellipsoidal geometry of the bundles. To this purpose, the Eshelby's tensor for an ellipsoid inclusion with symmetric axis x_3 has been used, whose expression is given by:

$$S_{22} = S_{33} = \begin{cases} \dfrac{\alpha}{2\left(\alpha^2-1\right)^{3/2}}\left[\alpha\left(\alpha^2-1^{1/2}\right)-\cosh^{-1}\alpha\right]; & \alpha \geq 1 \\ \dfrac{\alpha}{2\left(\alpha^2-1\right)^{3/2}}\left[cos^{-1}\alpha-\alpha\left(1-\alpha^2\right)^{1/2}\right]; & \alpha \geq 1 \end{cases} \tag{27}$$

with α the aspect ratio of the ellipsoid (a_1/a_2) and S_{11}=1 − 2S_{22}.

5. Results and discussion

In this section, the proposed analytical model is tested against experimental data from MWCNT reinforced cement paste, mortar and concrete experimental specimens. Moreover, the influence of the different variables affecting the overall electrical conductivity is also examined. In our calculations, the electrical conductivities of the three different matrices have been selected as 2.8×10^{-3} S/m, 1.04×10^{-3} S/m and 2.92×10^{-4} S/m, for cement paste (PA), cement mortar (MO) and concrete (CO), respectively [64, 65]. In order to compare the theoretical and experimental results, it must be taken into account the resistivity of the electrodes and the contact resistance [19]. Hence, an equivalent in series circuit with conductivity σ_{spc} has been defined, in which the resistivity of the electrodes and the contact resistance have been computed so that the initial plain configuration conductivity (f=0) is fitted. Having regard to the commercial specifications of MWCNTs (further discussed in the next section), the electrical conductivity of MWCNTs has been set in the range 10^0-10^7 S/m. The values of the constants used in the Simmon's model for the evaluation of the interphase conductivity in Eq. (2) are given in Table 1. For practical convenience, the concentration f of carbon nanotubes is usually expressed in the literature in terms of mass content with respect to weight of cement, w_{cem}, as follows:

$$w = \frac{\rho_N}{w_{cem}} f \tag{28}$$

with ρ_N being the density of the carbon nanotubes, taken as 150 kg/m^3, and w_{cem} the weight of cement in the composite.

Table 1: Physical constants used in Simmon's model

Mass of electron m	9.10938291×10^{-31} kg
Electric charge of an electron e	$-1.602176565\times10^{-19}$ C
Reduced Planck's constant $\hbar$	6.626068×10^{-34}m^{2}kg/s

5.1. Experiments

As discussed above, in order to validate the micromechanics model developed in the current work, the modeling results have been compared to the experimental data carried out in the specimens made of composite cement paste (PA), mortar (MO) and concrete (CO) doped with MWCNTs. Multi-walled carbon nanotubes type Graphistrength C100 from Arkema have been used as conductive nanoinclusions in the cementitious matrices. Table 2 reports the main physical, chemical and mechanical properties of the MWCNTs utilized for the nanocomposites' fabrication. Cement paste, mortar and concrete samples have been realized adding different quantities of MWCNTs, namely 0, 0.25, 0.5, 0.75, 1.0 and 1.5% with respect to the weight of cement. Table 3 summarizes the mix design of all the cementitious materials. Two different dispersant concentrations have been used, namely 1:1 and 10:1 with respect to the mass of the carbon nanotube fillers. The cement was pozzolanic, type 42.5. Sand and gravel had nominal dimensions between 0-4 mm and 4-8 mm, respectively. A plasticizer has been added to obtain similar workability for all the admixtures, with the same water/cement ratio of 0.45.

The cementitious samples were cube-shaped, with sides of 51 mm and five embedded stainless steel electrodes placed at a mutual distance of 10 mm. The electrodes were nets made of 0.5 mm diameter wires and mesh of 6 mm. In the case of concrete samples, the embedded part was modified, cutting alternatively the vertical wires, resulting in a final mutual distance of 12 mm. Figures 10(a) and 10(b) report the geometry of the specimens and of the electrodes, together with the picture of a cured sample. Figure 10(c) shows the setup of the experimental electrical tests carried out between two next electrodes at a distance of 10 mm, by use of a high precision LCR meter, model HM8018 [66].

Figure 11 sketches the preparation procedure for the paste, mortar and concrete samples with MWCNTs. In the first step the carbon nanotubes were added to the water solution with the surfactant through a preliminary mixing (Fig. 11(a) and 11(b)) and then were dispersed by use of a sonicator (Fig. 11(c)) or a mechanical stirrer (Fig. 11(c1)). After that, the obtained nano-modified suspension and the plasticizer were added to the cement

and mixed (Fig. 11(d)). The mixes were poured into oiled molds for curing, and the electrodes were embedded (Fig. 11(e)). After a few days, the samples were unmolded to complete the curing in controlled laboratory conditions (Fig. 11(f)). The dispersion and the morphology of MWCNTs in both water suspensions and cementitious materials were analyzed by use of SEM micrographs (Fig. 11(c1) and 11(f1)). SEM inspections have demonstrated that the MWCNTs dispersed in cementitious hardened matrices (paste, mortar and concrete) show wavy shapes similar to the ones observed after their dispersion in water solutions (Fig. 12).

Table 2: Main characteristics of MWCNTs used in the experiments (from Ref. [67])

Property	**Value**	**Property**	**Value**
Mean agglomerate size	200-500 μm	Apparent density	50-150 kg/m^3
Mean number of walls	5-15 μm	Weight loss at 105 °C	<1%
Outer mean diameter	10-15 nm	Thermal Conductivity	>3000 W/(mK)
Length	0.1-10 μm	Electric Conductivity	up to 10^7 $(\Omega m)^{-1}$
Carbon content	>90% in weight	Young Modulus	>1 TPa
Surface area	100-250 m$^2/g$	Tensile strength	About 150 GPa

Table 3: Mix designs of cementitious samples with six different concentrations of MWCNTs (the ratio ν between the mass of MWCNTs and cement varies from 0 to 1.5%). C_{0i} and C_i are the masses of cement in normal materials and with MWCNTs, respectively. ΔV_p, ΔV_m and ΔV_c are the total volumes of MWCNTs plus dispersant for paste, mortar and concrete nanomaterials, respectively, while η is the ratio between dispersant and MWCNTs, equal to 1 or to 10. [66].

Components	**Paste kg/m^3**		**Mortar kg/m^3**		**Concrete kg/m^3**	
	Normal	**With MWCNTs**	**Normal**	**With MWCNTs**	**Normal**	**With MWCNTs**
Cement 42.5N	C_{0p}=1277	$C_p=C_{0p}\frac{1m^3}{1m^3+\Delta V_p}$	C_{0m}=654	$C_m=C_{0m}\frac{1m^3}{1m^3+\Delta V_m}$	C_{0c}=524	$C_c=C_{0c}\frac{1m^3}{1m^3+\Delta V_c}$
Water	W_{0p}=574	$0.45C_p$	W_{0m}=294	$0.45C_m$	W_{0c}=234	$0.45C_c$
MWCNTs	-	νC_p	-	νC_m	-	νC_c
Dispersant	-	$\eta\nu C_p$	-	$\eta\nu C_m$	-	$\eta\nu C_c$
Sand	-	-	1308	$2C_m$	951	$1.81C_c$
Gravel	-	-	-	-	638	$1.22C_c$
Plasticizer	-	Var	-	Var	2.62	Var
W/C ratio	0.45	0.45	0.45	0.45	0.45	0.45

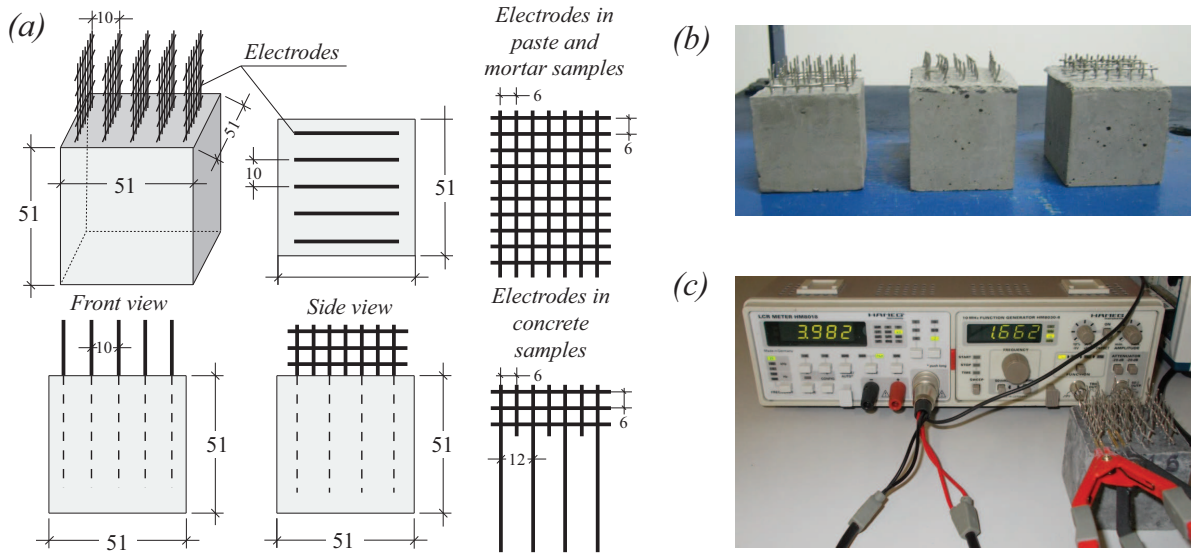

Figure 10: Geometry and dimensions of the cementitious samples and of the electrodes (a), picture of some samples with the embedded electrodes (b) and setup of the experimental electrical tests (c) (Units in mm).

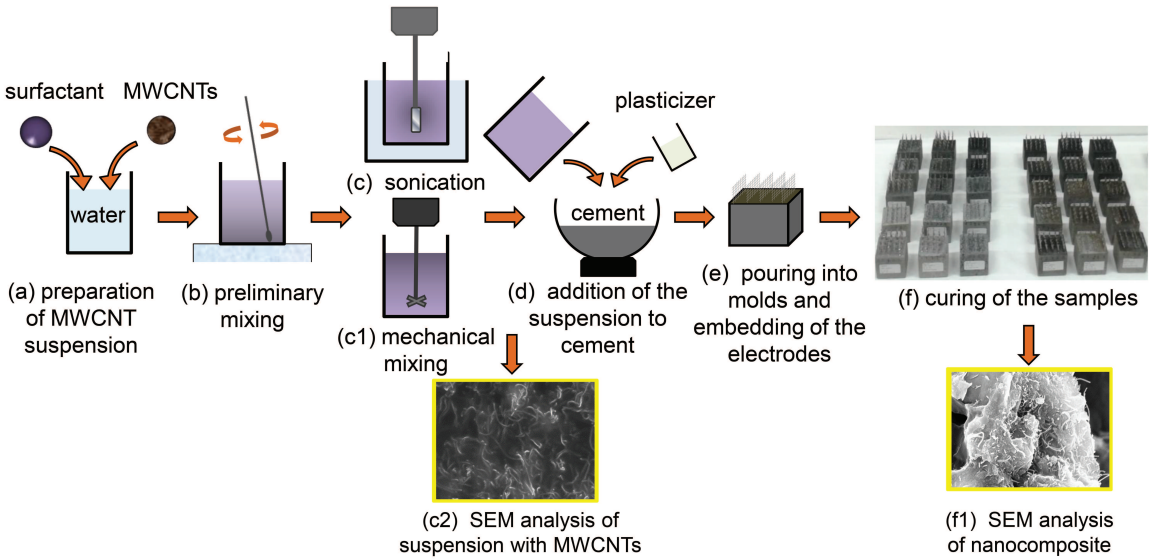

Figure 11: Preparation procedure of paste, mortar and concrete samples with MWCNTs.

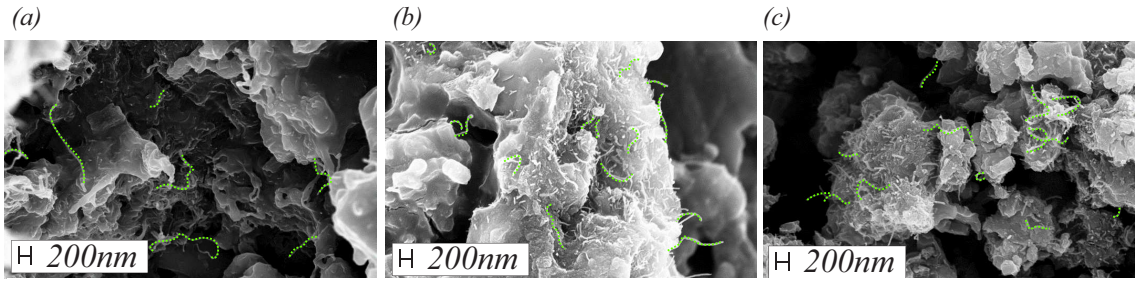

Figure 12: SEM pictures of MWCNTs dispersed using the SLS dispersant and sonicated with the SLS dispersant in the 1:1 (a) and 10:1 (b) amounts, and mechanically mixed using the SLS dispersant in the 10:1 amount (c).

5.2. Effects of constituents properties

Firstly, we have investigated the effects of CNTs aspect ratio, i.e. diameter and length, on the overall electrical conductivity of MWCNT-cement paste nanocomposites as shown in Figs. 13(a) and 13(b), respectively. It can be observed that both quantities have a significant effect on the percolating phase, while a moderate effect is found after percolation. The overall electrical conductivity increases with the increase in MWCNT length or the decrease in MWCNT diameter. This behavior is attributed to the greater likelihood of forming conductive networks of fibers with larger aspect ratio. Furthermore, it is observed that a reduction of the carbon nanotubes length results in an increase in the percolation threshold, while a reduction of the fibers diameters produces the opposite effect. It can be concluded from these results that the electrical conductivity of MWCNT-cement based specimens can be enhanced with the addition of carbon nanotubes with higher aspect ratio.

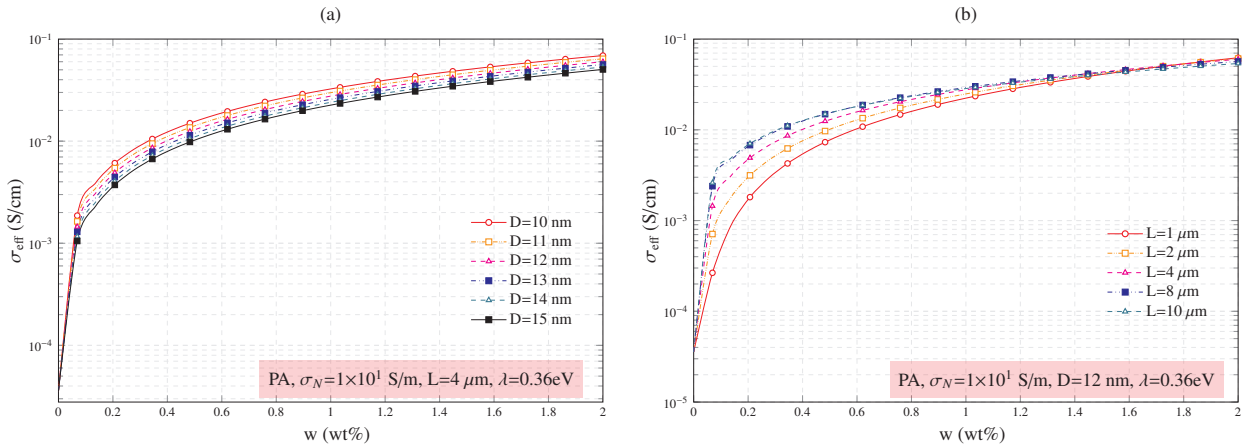

Figure 13: Effect of MWCNTs diameter (a) and length (b) on the electrical conductivity of MWCNT-cement paste nanocomposites.

In Fig. 14, it is shown the electrical conductivity of MWCNT-cement nanocomposites for different matrix materials, namely cement paste, mortar and concrete. It can be seen that, for every MWCNT concentration, the cement paste composites exhibit the highest values of conductivity whereas the concrete composites are the least conductive, circumstance that matches well the experimental experience. A key aspect of the electrical behavior of cement-based carbon nanotube composites is the uniformity of the dispersion of the nanoinclusions. As discussed above, different types of dispersants were employed for this purpose during the experimental campaign. It has been reported in the literature that dispersants create a partially isolating coating on the carbon nanotubes which can even inhibit the contact between the fibers [68]. This effect can be interpreted as an increment in the height of the tunneling potential barrier λ and, therefore, a reduction of the electron hopping contribution. Fig. 15 shows the electrical conductivity of MWCNT-cement paste nanocomposites with different values of λ. It is evidenced in this figure that the potential barrier height λ has substantial effect on the overall electrical conductivity of the composite before percolation. Higher values of λ lead to higher percolation thresholds, while limited differences are found after percolation. It can be extracted from this analysis that the employment of dispersant delays the percolation process, exhibiting more acute effects for MWCNTs concentration below percolation threshold.

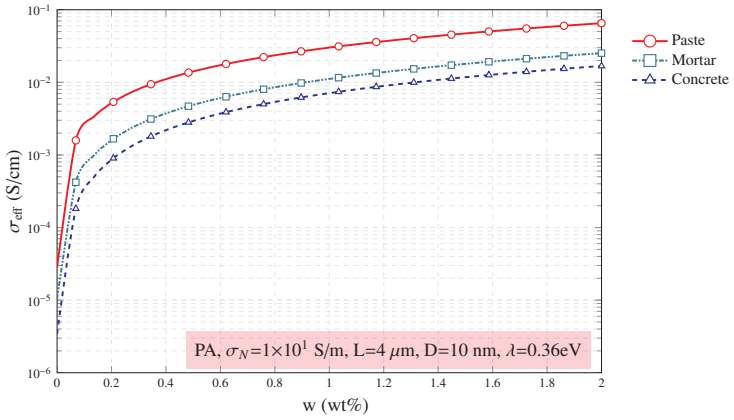

Figure 14: Electrical conductivity of MWCNT nanocomposites with different matrix materials: cement paste, mortar and concrete.

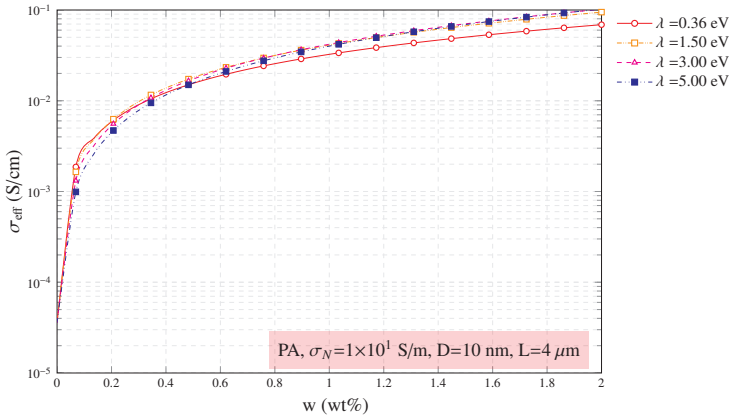

Figure 15: Effect of the electric potential barrier λ on the electrical conductivity of MWCNT-cement paste nanocomposites.

Fig. 16(a) demonstrates the effects of MWCNTs electrical conductivity σ_c on the overall conductivity of MWCNT cement paste nanocomposites. The analytical results obtained without considering the contribution of the conductive networks mechanism (CN) is also represented for illustrative purposes. It can be seen that, for low MWCNT concentrations before percolation, little differences are found among the modeling results with and without conductive network mechanism. Nevertheless, once the percolation threshold is reached, the conductive network mechanism becomes dominant and thus big differences appear between these two models. The predicted results are also compared to the experimental data in Fig. 16(b). In this first comparison, large differences are found among the experimental and theoretical results. The analytical estimations of the overall electrical conductivity are noticeably larger than the measurements carried out in the specimens. Furthermore, it can also be noticed that the percolation process predicted by the micromechanics modeling takes place before what is registered in the experimental specimens. The origin of these discrepancies may be attributed to waviness and agglomeration effects as it is shown in the following analyses.

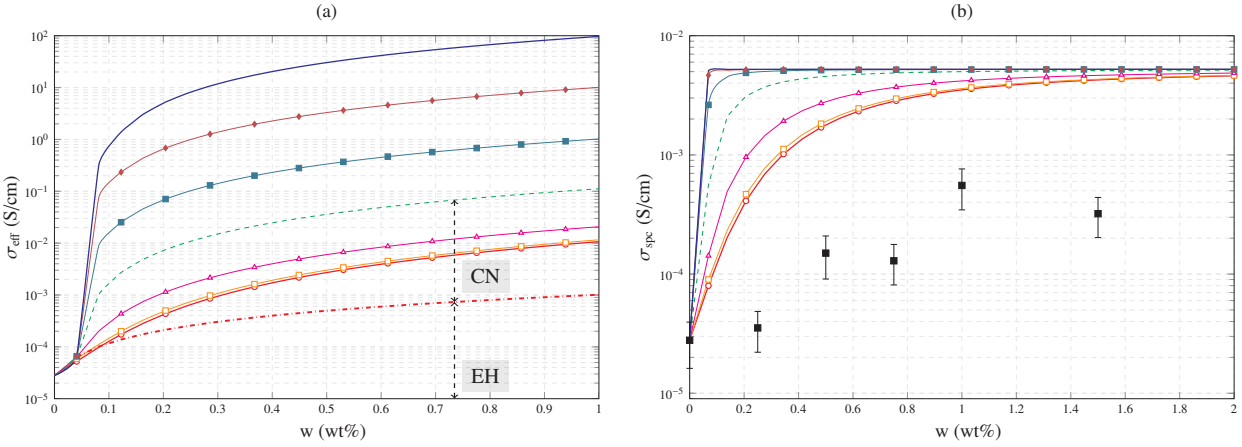

Figure 16: Effect of MWCNTs electrical conductivity σ_c on the effective conductivity of MWCNT-cement paste nanocomposites (a), and comparison with experimental data (b) (PA-SO-N%-6-1:1; λ=1.5eV; L = 1 μm; D = 15 nm; σ_c=1e-2 S/cm; σ_c=1e-1 S/cm; σ_c=1e+0 S/cm; σ_c=1e+1 S/cm; σ_c=1e+2 S/cm; σ_c=1e+3 S/cm; σ_c=1e+4 S/cm; σ_c=1e+1 S/cm (No conductive networks); ■ experimental data; the error bars denote ± standard deviation intervals, with standard deviations computed by varying the electrodes).

5.3. Effects of MWCNTs waviness

In this section, the effect of MWCNTs waviness is investigated. The comparison analysis of Fig. 16(b) is here updated for the case of σ_c=1e+0 S/cm with four wavy geometries, corresponding to helical angles of 90, 80, 60 and 30°, as represented in Fig. 17(b). It can be seen in Fig. 17(a) that the main effect of non-straightness of the fibers is a delay of the percolation process. This effect is attributed to the reduction of the length from wavy to equivalent straight fiber, what leads to an increment of the percolation threshold. However, the electrical conductivity predicted by the micromechanics modeling is still larger than the experimental data. This difference may be due to imperfections associated with a non-uniform nanoinclusions distribution, namely agglomeration.

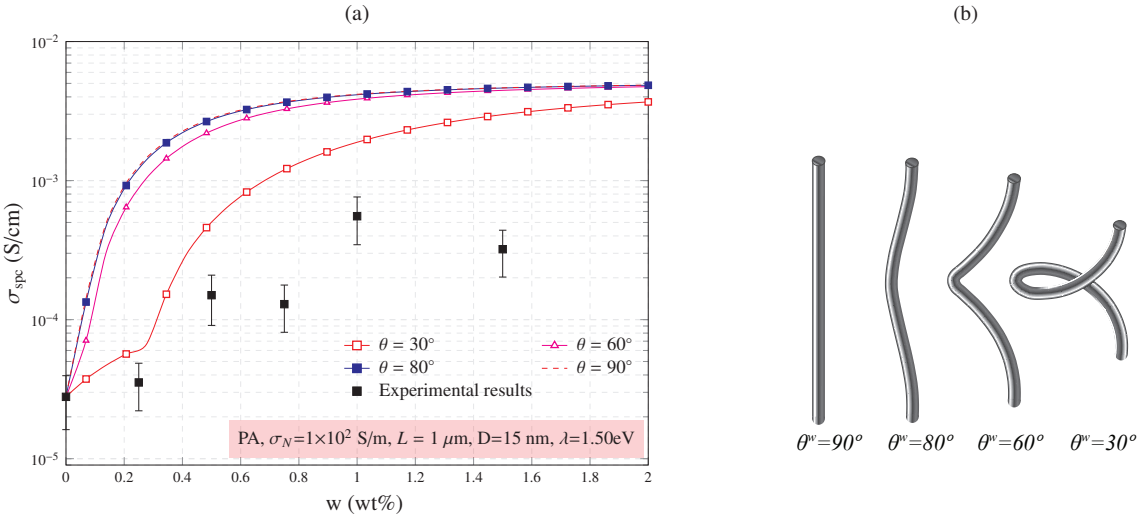

Figure 17: Effect of the MWCNT waviness on the electrical conductivity of the MWCNT cement paste nanocomposite (PA-SO-N%-6-1:1); the error bars denote ± standard deviation intervals, with standard deviations computed by varying the electrodes.

5.4. Effects of MWCNTs agglomeration

The effect of MWCNTs agglomeration in spherical bundles on the conductivity of cement-based composites has been also analyzed. In Figs. 18(a) and 18(b) it is shown the overall conductivity for different agglomeration parameters χ and ζ, respectively. It is extracted from this analysis that the nanoinclusions distribution has a strong influence on the overall conductivity of the composite. In Fig. 18(a), the volume fraction of MWCNTs within the bundles is set at 90% (ζ = 0.9), whereas the ratio between the volume of the bundles and the total volume of the RVE varies from 10 to 90%. It can be noticed that the percolation process takes place sequentially within and outside the bundles. At the contrary, in Fig. 18(b) the volume fraction of the bundles is set at 40% and the ratio of MWCNTs concentration within them ranges from 40 to 90%. The higher is the concentration of MWCNTs within the clusters, the lesser is the nanoinclusions uniformity and, thus, the lesser is the overall conductivity of the composite. Different geometries of bundles are also investigated in Fig. 19. In particular, aspect ratios a_1/a_3=1, 2, 3 and 4 have been studied. It is concluded that spherical bundles lead to the lowest electrical conductivity, while higher aspect ratios exhibit higher values.

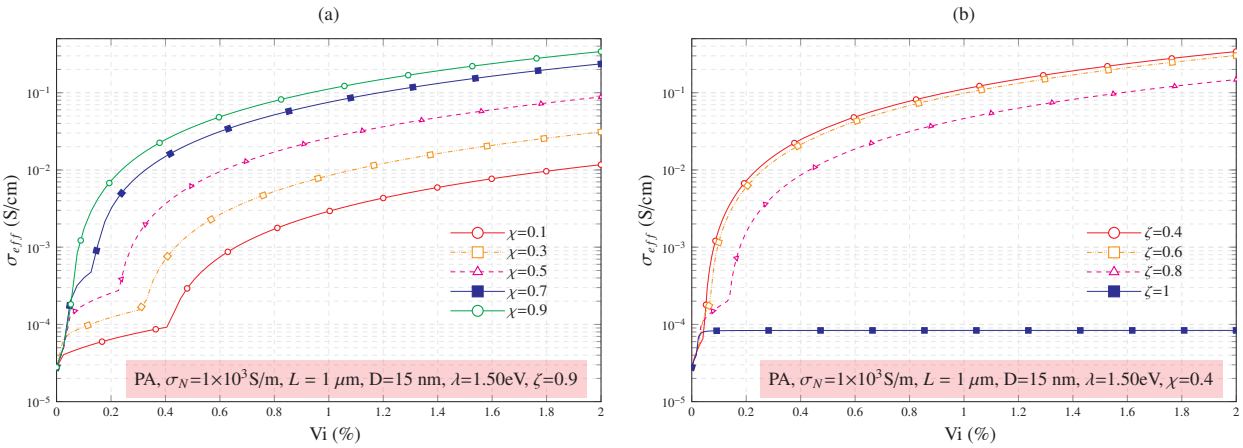

Figure 18: Effect of the MWCNTs agglomeration on the electrical conductivity of the MWCNT cement paste nanocomposite (a_1/a_3 = 1).

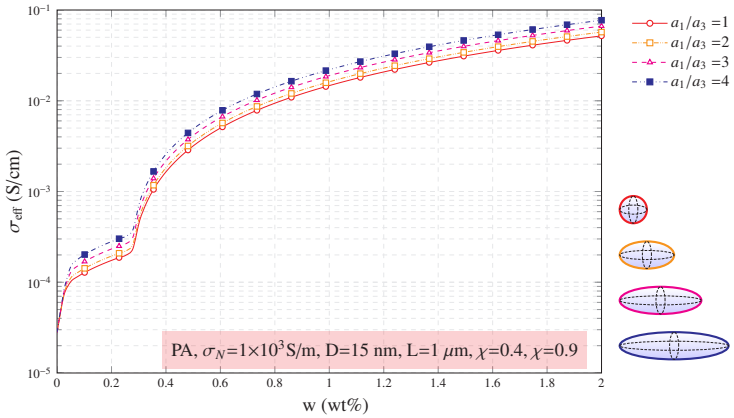

Figure 19: Effect of aspect ratio of ellipsoidal bundles (a_1/a_3) on the electrical conductivity of MWCNT-cement paste nanocomposites.

The combination of waviness and clustering can give an explanation of the differences observed in the comparison analysis of Fig. 16, which was carried out under the assumption of straight uniformly distributed MWCNTs. Fig. 20 shows the comparison between the experimental data and the analytical results considering wavy MWCNTs ($\theta = 50°$) and non-uniform spatial distribution ($\chi = 0.3$; $\xi = 0.8$). It can be seen that the coupled effect of waviness and clustering can lead to more realistic estimates with closer agreements with the experimental data.

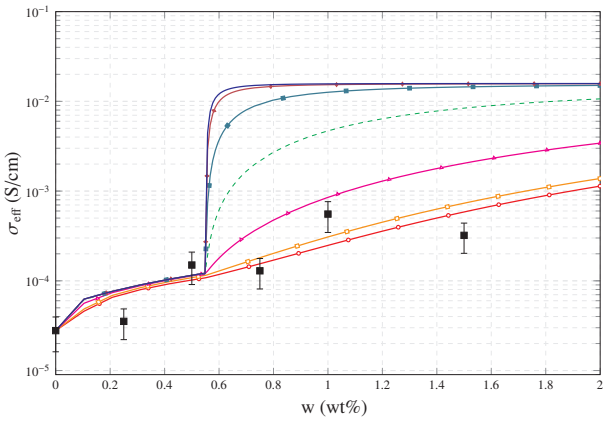

Figure 20: Comparison between modeling results and experimental data for a wavy non-uniform MWCNT-cement paste nanocomposite (PA-SO-N%-6-1:1; λ=1.5eV; $L = 1$ μm; $D = 15$ nm; $\theta = 35°$; $\chi = 0.2$; $\zeta = 0.7$; σ_c=1e-2 S/cm; σ_c=1e-1 S/cm; σ_c=1e+0 S/cm; σ_c=1e+1 S/cm; σ_c=1e+2 S/cm; σ_c=1e+3 S/cm; σ_c=1e+4 S/cm; ■ experimental data; the error bars denote ± standard deviation intervals, with standard deviations computed by varying the electrodes).

5.5. Comparison analyses with cement-based specimens

On the basis of the previous analyses, the proposed micromechanics approach is compared to the experimental results obtained for different cement-based composites, namely cement paste, cement mortar and concrete. Fig. 21 shows the comparison between the modeling results and the experimental data for different matrix materials and manufacturing processes. The waviness of the MWCNTs has been defined with a spiral angle of 50° in all cases except for sonicated specimens with high dispersant concentrations (10:1). It is found that the analytical results agree well with the experimental data when the CNT electrical conductivity are set between 100 S/m and 1000 S/m. It can be seen that generally the addition of larger dispersant concentrations can be simulated with larger agglomeration parameters. Furthermore, the incorporation of dispersant acts as a partially isolating coating on the surface of the nanotubes, what has been simulated by an increment of the potential barrier λ. In particular values of 1.5 and 3eV have been taken for the cases of low (1:1) and high dispersant (10:1) concentration, respectively. The influence of the manufacturing process, sonication (SO) or mechanical (ME), has been taken into account via different agglomeration parameters, generally stricter in the case of mechanical mixing. It is noticeable the cases of cement paste and mortar specimens in which the dispersant has a special effect on the uniformity of the composite. In these cases, the absence of gravel reduces the advantages of sonication with respect to mechanical mixing,

leading to more uniform dispersions of nanotubes with mechanical mixing and high dispersant concentration than with sonication and low dispersant concentrations.

The experimental results also reveal abrupt decreases in the electrical conductivity with respect to the plain material for specimens with high dispersant concentration and low MWCNTs content (see, e.g., Figs. 21(e) and 21(f)). This phenomenon may be caused by the formation of a partially isolating coating on the surface of the nanotubes induced by the dispersants. This isolating coating has been also reported in the literature [68] in terms of the formation of surfactant-induced electromechanical double-layers (polarization resistance), what may make the nanotubes behave as non-conductive fibers when their separation distances are large. However, as the content of nanotubes increases, the separation distance decreases and this effect is canceled. In the present work, attempts have been made to simulate this effect by means of reductions of the conductivity of the equivalent solid cylinders at low MWCNT concentrations. Nonetheless, this approach was insufficient to reproduce these falls of the electrical conductivity. Hence, it is hypothesized that the employment of high concentrations of dispersants at low MWCNT concentrations, does not only isolate the nanoinclusions but may also increase the resistivity of the matrix and the contact resistance. Further research is needed on this issue in order to count on more accurate models of MWCNT cement-based materials with high dispersant concentration doped with low MWCNTs contents.

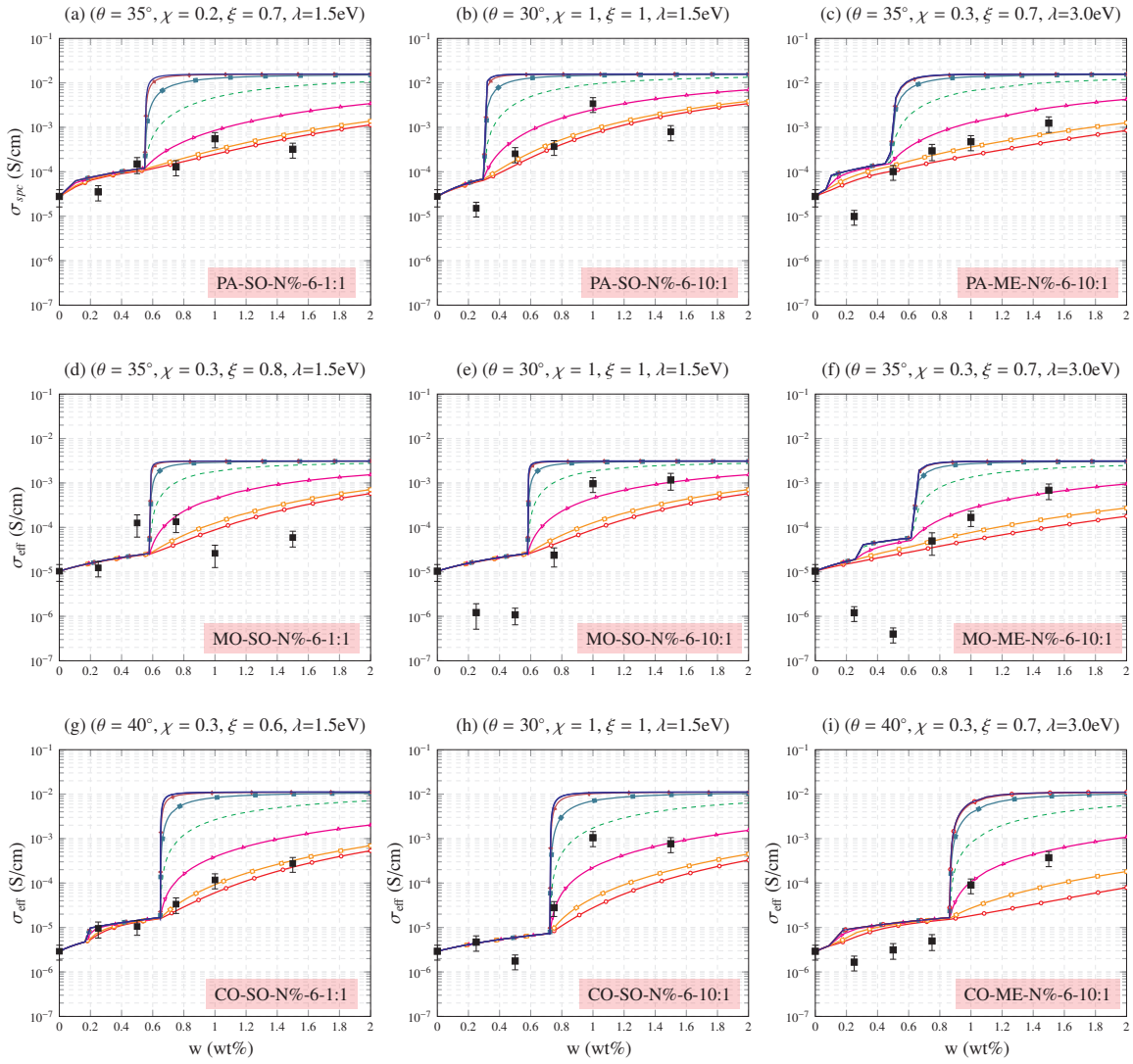

Figure 21: Comparison between modeling results and experimental data: composite pastes (a,b,c); composite mortars (d, e, f); composite concretes (g, h, i). (σ_c=1e+0 S/m; σ_c=1e+1 S/m; σ_c=1e+2 S/m; σ_c=1e+3 S/m; σ_c=1e+4 S/m; σ_c=1e+5 S/m; σ_c=1e+6 S/m; ■ experimental data; the error bars denote ± standard deviation intervals, with standard deviations computed by varying the electrodes; L = 1 μm; D = 15 nm).

5.6. Sensitivity analyses

Finally, in order to assess the propagation of potential statistical randomness in the design variables on the overall electrical conductivity of MWCNT cement-based composites, an input sensitivity analysis is presented.

A sensitivity analysis is defined as the study of the contribution of the variation of the input variables to the variation of the output of a model. In particular, the sensitivity of the effective electrical conductivity of two different MWCNTs concentrations has been analyzed, namely w=0.8% and 1.5%, as shown in Figs. 22 and 23, respectively. The input variables have been categorized in constituents properties $\{L, D, \sigma_m, \sigma_c\}$, waviness $\{\theta\}$ and agglomeration $\{\chi, \zeta\}$. Defining an independent input variation of 20% with respect to the initial value, the sensitivity coefficient S_σ with respect to an input variable x can be computed as follows:

$$S_\sigma(\%) = 100 \frac{\Delta\sigma_{eff}}{\Delta x} \frac{x}{\sigma_{eff}} \tag{29}$$

The first study (Fig. 22) represents the sensitivity analysis of a MWCNTs content close to the percolation threshold. In this case, it is observed that the most influential variable is the conductivity of the matrix. A significant effect of the fiber aspect ratio, i.e. length and diameter, is also found as well as a considerable contribution of the helical waviness. It is also noticeable the limited influence of the agglomeration parameters and an almost null sensitivity due to variation of the conductivity of the nanotubes. Likewise, the second case (Fig. 23) analyzes the sensitivity of the overall conductivity with a MWCNT content far from the percolation threshold. It is noticed here that the aspect ratio of the MWCNTs becomes predominant. Moreover, once some conductive paths are formed, the conductivity of the matrix loses relevance and, conversely, the waviness gains importance.

In the light of these last results, the comparison between the analytical and experimental data has been updated treating the main variables as random, namely $\{L, D, \sigma_m, \theta\}$, and neglecting the variation of the conductivity of the nanotubes σ_c and the agglomeration parameters, χ and ζ. A random variation of 5% has been considered for all the cited variables with respect to their mean value. Fig. 24(a) represents a scatter plot of the overall electrical conductivity of concrete with low dispersant concentration with respect to the MWCNT concentration. This result remarks a stronger influence of the variation of the variables on the overall conductivity for filler concentrations above the percolation threshold, where the dispersion of the results is higher. In Fig. 24(b), these results are compared to the experimental data. The max/min band of the experimental data is also represented. It can be noticed that most of the analytical results lie within the experimental band, what demonstrates a further validation of the proposed approach and the feasibility of developing further stochastic analyses in future works.

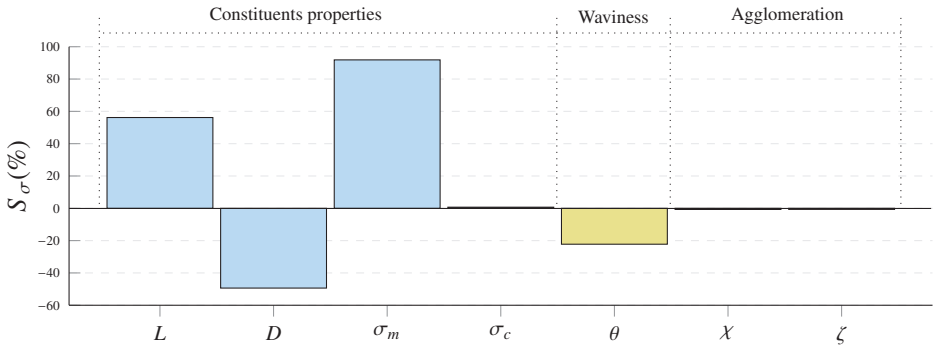

Figure 22: Sensitivity analysis of the overall electrical conductivity of MWCNTs cement paste nanocomposites with respect to the variation of the main variables associated with constituents properties, waviness and agglomeration (w=0.8%, σ_c=1e+4 S/m, $L = 2\ \mu$m, $D = 10$ nm, λ=0.36eV, $\theta = 90°$, $\chi = 0.4$, $\xi = 0.4$)

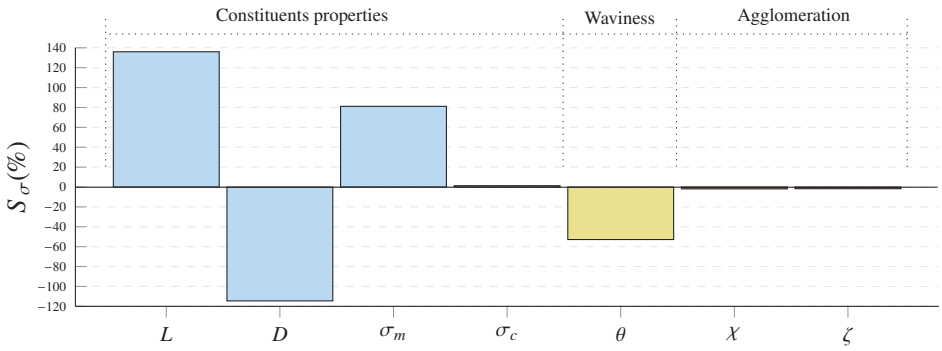

Figure 23: Sensitivity analysis of the overall electrical conductivity of MWCNTs cement paste nanocomposites with respect to the variation of the main variables associated with constituents properties, waviness and agglomeration (w=1.5%, σ_c=1e+4 S/m, $L = 2\ \mu$m, $D = 10$ nm, λ=0.36eV, $\theta = 90°$, $\chi = 0.4$, $\xi = 0.4$)

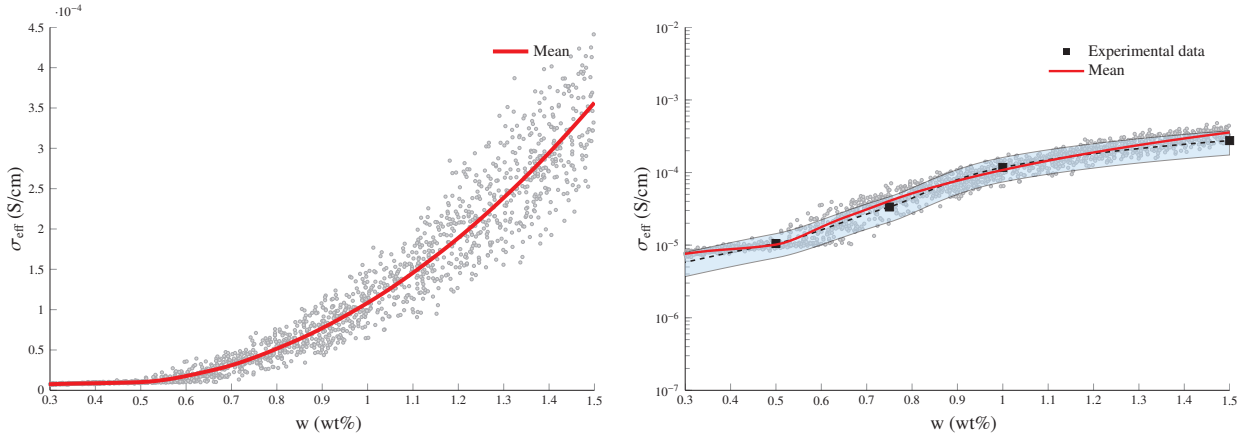

Figure 24: Scatter plot of the overall electrical conductivity of MWCNTs cement paste nanocomposites for random simultaneous variation of 5% with respect to the mean value of the parameters $\{L, D, \sigma_m, \theta\}$; (a) analytic overall electrical conductivity in linear scale, (b) Comparison between the analytical results and the max/min experimental band data in logarithmic scale (CO-SO-N%-6-1:1, σ_c=1e+1 S/m, $\overline{L} = 1\ \mu$m, $\overline{D} = 15$ nm, λ=1.5eV, $\overline{\theta} = 40°$, $\chi = 0.14$, ξ=0.42).

6. Conclusions

This paper has presented a micromechanics model to predict the overall conductivity of CNT cement-based nanocomposites with the consideration of waviness and non-uniform spatial distributions of nanoinclusions. The two mechanisms that contribute to the conductivity of CNT composites, namely electron hopping and conductive networks, have been contemplated in the mixed micromechanics framework. The electron hopping mechanism, corresponding to a quantum tunneling phenomenon, has been simulated through a conductive interphase surrounding the nanotubes, whereas the conductive networks mechanism has been modeled by means of changes on the aspect ratios of fibers. Moreover, a helical waviness model and a two-parameter agglomeration approach have been proposed, for the first time, on the basis of SEM inspections.

In order to count on an experimental basis to use as benchmark to validate the analytical model, several nanocomposite cement-based specimens have been manufactured and tested. In particular, specimens of cement pastes, mortars and concretes with different concentrations of MWCNTs have been prepared using three specific preparation techniques. The first one consists of using a high amount of dispersant and mechanical mixing. The two remaining strategies consider similar and lower dispersant concentrations with ultrasonic treatment. The quality of the dispersion has been evaluated using scanning electron microscopy.

Detailed parametric analyses have been carried out in order to illustrate the influence of the constituents properties, waviness and agglomeration. In order to evaluate the possible effects of the employment of dispersants on the contact among nanotubes, the influence of the variation of the height of the tunneling potential barrier has been analyzed. Furthermore, the effects of non-uniform spatial distributions of MWCNTs have been evaluated through the proposed two-parameters agglomeration model. By means of the proposed ellipsoidal geometry of the bundles , the effect of different cluster aspect ratios have been investigated. Finally, the accuracy of the proposed approach

has been proved by comparison with the experimental data from the tested specimens. In addition, two sensitivity analyses of the effective conductivity of the composites with MWCNT content close and far from the percolation threshold, respectively, have been presented in order to gain some insight into the structure of the proposed model.

The main contributions of this paper are summarized below.

- The overall electrical conductivity of MWCNT cement-based composites is governed by the simultaneous contribution of the electron hopping and conductive networks mechanisms. The analysis of the effects of the conductivity of the MWCNTs remarks a dominant role of the conductive network mechanism above the percolation process.
- The parametric analyses highlight the importance of the aspect ratio of the nanotubes for the design of MWCNTs nanocomposites. Increments of the length and reductions of the diameter, i.e. increments of the aspect ratio, lead to decrements in the percolation threshold and, therefore, higher likelihood of forming conductive paths.
- The analytical predictions show that the nanoinclusions distribution has a strong influence on the overall conductivity of the composite. The results reveal that the higher is the concentration of MWCNTs within the clusters, the lesser is the nanoinclusions uniformity and, thus, the lesser is the overall conductivity of the composite.
- The comparison of the analytical predictions against experimental data demonstrates that the consideration of straight uniformly distributed MWCNTs leads to overestimated conductivity. On the contrary, it is shown that the incorporation of waviness and agglomeration effects, on the basis of SEM inspections, provides closer fits to the experimental data. Hence, it is concluded that the wavy state of the fibers as well as their agglomeration in bundles play a key-role in the conductivity of cement-based nanocomposites.
- The sensitivity analysis shows that, in the case of MWCNT content close to the percolation threshold, the most influential variable in the sensitivity of the overall electrical conductivity of the composite is the conductivity of the matrix. A significant effect of the fiber aspect ratio is also found as well as a considerable contribution of the helical waviness. It is also noticeable the limited influence of the agglomeration parameters and an almost negligible role played by the conductivity of the nanotubes. On the contrary, in the case of MWCNTs content above the percolation threshold, the aspect ratio of the MWCNTs becomes predominant. Moreover, once some conductive paths are formed, the conductivity of the matrix loses relevance and, conversely, the waviness gains importance.

The presented micromechanics model is envisaged to provide a useful tool for the understanding of the physical mechanisms that govern the electrical conductivity of MWCNT cement-based composites. Furthermore, this analytical approach generates quantitative predictions, valuable for the design of these composites with a reduced computational cost. Finally, this model gives an analytical framework suitable for the incorporation of uncertainty of the constituents properties, waviness and agglomeration, interesting for future further researches on stochastic design of MWCNT cement-based composites. Further developments taking account of the heterogeneous nature of cement-based matrices needs to be pursued in order to enhance the accuracy of the predictions. An extension of the proposed method with a multi-inclusion approach would allow to consider relevant aspects such as granulometry, moisture, hydration processes and environmental temperature.

Acknowledgement

This work was partially financed by the Ministerio de Economía y Competitividad of Spain under the project DPI2014-53947-R. It is also gratefully acknowledged the support of Regione Umbria, within POR Umbria ESF 2007-2013, Axis II Employability - Objective and Axis IV Human - Capital Objective l. E. G-M was also supported by a FPU contract-fellowship from the Spanish Ministry of Education Ref: FPU13/04892. The support of the Italian Ministry of Education, University and Research (MIUR) through the funded Project of Relevant National Interest "SMART-BRICK: Novel strain-sensing nano-composite clay brick enabling self-monitoring masonry structures" is also gratefully acknowledged.

References

[1] B. I. Yakobson, P. Avouris, Mechanical properties of carbon nanotubes, in: Carbon nanotubes, Springer, 2001, pp. 287–327.

[2] B. Demczyk, Y. Wang, J. Cumings, M. Hetman, W. Han, A. Zettl, R. Ritchie, Direct mechanical measurement of the tensile strength and elastic modulus of multiwalled carbon nanotubes, Materials Science and Engineering: A 334 (2002) 173–178.

[3] T. Ebbesen, H. Lezec, H. Hiura, J. Bennett, H. Ghaemi, T. Thio, Electrical conductivity of individual carbon nanotubes, Nature 382 (1996) 54–56.

[4] E. T. Thostenson, Z. Ren, T. W. Chou, Advances in the science and technology of carbon nanotubes and their composites: a review, Composites science and technology 61 (2001) 1899–1912.

[5] B. Han, X. Yu, E. Kwon, A self-sensing carbon nanotube/cement composite for traffic monitoring, Nanotechnology 20 (2009) 445501.

[6] F. Ubertini, A. L. Materazzi, A. D'Alessandro, S. Laflamme, Natural frequencies identification of a reinforced concrete beam using carbon nanotube cement-based sensors, Engineering Structures 60 (2014) 265–275.

[7] B. Han, Y. Wang, S. Dong, L. Zhang, S. Ding, X. Yu, J. Ou, Smart concretes and structures: A review, Journal of intelligent material systems and structures 26 (2015) 1303–1345.

[8] A. Sobolkina, V. Mechtcherine, V. Khavrus, D. Maier, M. Mende, M. Ritschel, A. Leonhardt, Dispersion of carbon nanotubes and its influence on the mechanical properties of the cement matrix, Cement and Concrete Composites 34 (2012) 1104–1113.

[9] R. Siddique, A. Mehta, Effect of carbon nanotubes on properties of cement mortars, Construction and Building Materials 50 (2014) 116–129.

[10] B. Chen, K. Wu, W. Yao, Conductivity of carbon fiber reinforced cement-based composites, Cement and Concrete Composites 26 (2004) 291–297.

[11] M. Chiarello, R. Zinno, Electrical conductivity of self-monitoring CFRC, Cement and Concrete Composites 27 (2005) 463–469.

[12] S. Wen, D. Chung, Double percolation in the electrical conduction in carbon fiber reinforced cement-based materials, Carbon 45 (2007) 263–267.

[13] S. Wen, D. Chung, Carbon fiber-reinforced cement as a thermistor, Cement and Concrete Research 29 (1999) 961–965.

[14] H. Li, H. G. Xiao, J. P. Ou, Effect of compressive strain on electrical resistivity of carbon black-filled cement-based composites, Cement and Concrete Composites 28 (2006) 824–828.

[15] L. Chang, K. Friedrich, L. Ye, P. Toro, Evaluation and visualization of the percolating networks in multi-wall carbon nanotube/epoxy composites, Journal of materials science 44 (2009) 4003–4012.

[16] B. Han, B. Han, X. Yu, Experimental study on the contribution of the quantum tunneling effect to the improvement of the conductivity and piezoresistivity of a nickel powder-filled cement-based composite, Smart Materials and Structures 18 (2009) 065007.

[17] B. Han, S. Ding, X. Yu, Intrinsic self-sensing concrete and structures: A review, Measurement 59 (2015) 110–128.

[18] H. Li, H. G. Xiao, J. P. Ou, A study on mechanical and pressure-sensitive properties of cement mortar with nanophase materials, Cement and Concrete research 34 (2004) 435–438.

[19] B. Han, X. Guan, J. P. Ou, Electrode design, measuring method and data acquisition system of carbon fiber cement paste piezoresistive sensors, Sensors and Actuators A: Physical 135 (2007) 360–369.

[20] B. Han, B. Han, J. Ou, Experimental study on use of nickel powder-filled portland cement-based composite for fabrication of piezoresistive sensors with high sensitivity, Sensors and Actuators A: Physical 149 (2009) 51–55.

[21] A. D'Alessandro, F. Ubertini, A. L. Materazzi, S. Laflamme, M. Porfiri, Electromechanical modelling of a new class of nanocomposite cement-based sensors for structural health monitoring, Structural Health Monitoring (2014) 1475921714560071.

[22] B. Han, K. Zhang, X. Yu, E. Kwon, J. Ou, Electrical characteristics and pressure-sensitive response measurements of carboxyl MWNT/cement composites, Cement and Concrete Composites 34 (2012) 794–800.

[23] M. E. Newman, R. M. Ziff, Fast monte carlo algorithm for site or bond percolation, Physical Review E 64 (2001) 016706.

[24] H. Ma, X. L. Gao, A three-dimensional monte carlo model for electrically conductive polymer matrix composites filled with curved fibers, Polymer 49 (2008) 4230–4238.

[25] T. Zhang, Y. Yi, Monte carlo simulations of effective electrical conductivity in short-fiber composites, Journal of applied physics 103 (2008) 014910.

[26] W. Lu, T. W. Chou, E. T. Thostenson, A three-dimensional model of electrical percolation thresholds in carbon nanotube-based composites, Applied Physics Letters 96 (2010) 223106.

[27] S. Kirkpatrick, Percolation and conduction, Reviews of modern physics 45 (1973) 574.

[28] G. Grimmett, Percolation Springer-Verlag, Berlin (Second edition) (1999).

[29] F. Deng, Q. S. Zheng, An analytical model of effective electrical conductivity of carbon nanotube composites, Applied Physics Letters 92 (2008) 071902.

[30] T. Takeda, Y. Shindo, Y. Kuronuma, F. Narita, Modeling and characterization of the electrical conductivity of carbon nanotube-based polymer composites, Polymer 52 (2011) 3852–3856.

[31] G. D. Seidel, D. C. Lagoudas, A micromechanics model for the electrical conductivity of nanotube-polymer nanocomposites, Journal of Composite Materials 43 (2009) 917–941.

[32] T. Mori, K. Tanaka, Average stress in matrix and average elastic energy of materials with misfitting inclusions, Acta metallurgica 21 (1973) 571–574.

[33] H. Hatta, M. Taya, Effective thermal conductivity of a misoriented short fiber composite, Journal of Applied Physics 58 (1985) 2478–2486.

[34] C. Feng, L. Jiang, Micromechanics modeling of the electrical conductivity of carbon nanotube (CNT)–polymer nanocomposites, Composites Part A: Applied Science and Manufacturing 47 (2013) 143–149.

[35] M. S. Shaffer, A. H. Windle, Fabrication and characterization of carbon nanotube/poly (vinyl alcohol) composites, Advanced materials 11 (1999) 937–941.

[36] B. Vigolo, A. Penicaud, C. Coulon, C. Sauder, R. Pailler, C. Journet, P. Bernier, P. Poulin, Macroscopic fibers and ribbons of oriented carbon nanotubes, Science 290 (2000) 1331–1334.

[37] R. H. Poelma, X. Fan, Z. Y. Hu, G. Van Tendeloo, H. W. van Zeijl, G. Q. Zhang, Effects of nanostructure and coating on the mechanics of carbon nanotube arrays, Advanced Functional Materials 26 (2016) 1233–1242.

[38] Y. Yi, L. Berhan, A. Sastry, Statistical geometry of random fibrous networks, revisited: waviness, dimensionality, and percolation, Journal of applied physics 96 (2004) 1318–1327.

[39] L. Berhan, A. Sastry, Modeling percolation in high-aspect-ratio fiber systems. II. the effect of waviness on the percolation onset, Physical Review E 75 (2007) 041121.

[40] F. Fisher, R. Bradshaw, L. Brinson, Fiber waviness in nanotube-reinforced polymer composites: Modulus predictions using effective nanotube properties, Composites Science and Technology 63 (2003) 1689–1703.

[41] C. Li, E. T. Thostenson, T. W. Chou, Effect of nanotube waviness on the electrical conductivity of carbon nanotube-based composites, Composites Science and Technology 68 (2008) 1445–1452.

[42] A. Allaoui, S. Bai, H.-M. Cheng, J. Bai, Mechanical and electrical properties of a MWNT/epoxy composite, Composites Science and Technology 62 (2002) 1993–1998.

[43] H. Li, H. G. Xiao, J. Yuan, J. P. Ou, Microstructure of cement mortar with nano-particles, Composites Part B: Engineering 35 (2004) 185–189.

[44] J. M. Wernik, S. A. Meguid, Recent developments in multifunctional nanocomposites using carbon nanotubes, Applied Mechanics Reviews 63 (2010) 050801.

[45] S. H. Jang, S. Kawashima, H. Yin, Influence of carbon nanotube clustering on mechanical and electrical properties of cement pastes, Materials 9 (2016) 220.

[46] G. J. Weng, A dynamical theory for the Mori–Tanaka and Ponte Castañeda–Willis estimates, Mechanics of Materials 42 (2010) 886–893.

[47] B. Yang, K. Cho, G. Kim, H. Lee, Effect of CNT agglomeration on the electrical conductivity and percolation threshold of nanocomposites: A micromechanics-based approach, CMES: Computer Modeling in Engineering & Sciences 103 (2014) 343–365.

[48] R. Wiesendanger, Scanning probe microscopy and spectroscopy: methods and applications, Cambridge University Press, 1994.

[49] R. W. Robinett, R. Murphy, Quantum mechanics: classical results, modern systems and visualized examples, American Journal of Physics 65 (1997) 1218–1218.

[50] S. Wen, D. Chung, Effect of carbon fiber grade on the electrical behavior of carbon fiber reinforced cement, Carbon 39 (2001) 369–373.

[51] J. Xu, W. Zhong, W. Yao, Modeling of conductivity in carbon fiber-reinforced cement-based composite, Journal of materials science 45 (2010) 3538–3546.

[52] A. Allaoui, S. V. Hoa, M. D. Pugh, The electronic transport properties and microstructure of carbon nanofiber/epoxy composites, Composites Science and Technology 68 (2008) 410–416.

[53] J. G. Simmons, Generalized formula for the electric tunnel effect between similar electrodes separated by a thin insulating film, Journal of Applied Physics 34 (1963) 1793–1803.

[54] C. Li, E. T. Thostenson, T. W. Chou, Dominant role of tunneling resistance in the electrical conductivity of carbon nanotube–based composites, Applied Physics Letters 91 (2007) 223114.

[55] K. Yan, Q. Xue, Q. Zheng, L. Hao, The interface effect of the effective electrical conductivity of carbon nanotube composites, Nanotechnology 18 (2007) 255705.

[56] J. D. Eshelby, The determination of the elastic field of an ellipsoidal inclusion, and related problems, Proceedings of the Royal Society of London. Series A. Mathematical and Physical Sciences 241 (1957) 376–396.

[57] J. Eshelby, The elastic field outside an ellipsoidal inclusion, Proceedings of the Royal Society of London. Series A, Mathematical and Physical Sciences (1959) 561–569.

[58] G. M. Odegard, T. S. Gates, Constitutive modeling of nanotube/polymer composites with various nanotube orientations, in: Proceedings Annual Conference on Experimental and Applied Mechanical.

[59] M. Taya, Electronic composites: modeling, characterization, processing, and MEMS applications, Cambridge University Press, 2005.

[60] L. Gao, Z. Li, Effective medium approximation for two-component nonlinear composites with shape distribution, Journal of physics: Condensed matter 15 (2003) 4397.

[61] C. Feng, Micromechanics Modeling of the Electrical Conductivity of Carbon Nanotude (CNT)-Polymer Nanocomposites, Ph.D. thesis, University of Western Ontario, 2014.

[62] M. Shiraishi, M. Ata, Work function of carbon nanotubes, Carbon 39 (2001) 1913–1917.

[63] D. L. Shi, X. Q. Feng, Y. Y. Huang, K. C. Hwang, H. Gao, The effect of nanotube waviness and agglomeration on the elastic property of carbon nanotube-reinforced composites, Journal of Engineering Materials and Technology 126 (2004) 250–257.

[64] A. M. Neville, Properties of concrete, 4th edition, 1995.

[65] Y. Liao, X. Wei, Penetration resistance and electrical resistivity of cement paste with superplasticizer, Materials and structures 47 (2014) 563–570.

[66] A. D'Alessandro, M. Rallini, F. Ubertini, A. L. Materazzi, J. M. Kenny, Investigations on scalable fabrication procedures for self-sensing carbon nanotube cement-matrix composites for SHM applications, Cement and Concrete Composites 65 (2016) 200–213.

[67] T. P. McAndrew, P. Laurent, M. Havel, C. Roger, Arkema graphistrength® multi-walled carbon nanotubes, Technical Proceedings of the 2008 NSTI Nanotechnology Conference and Trade Show, NSTI-Nanotech, Nanotechnology 2008 1 (2008) 47–50.

[68] S. Wansom, N. Kidner, L. Woo, T. Mason, AC-impedance response of multi-walled carbon nanotube/cement composites, Cement and Concrete Composites 28 (2006) 509–519.